Review

A Review on Oxygen-deficient Titanium Oxide for Photocatalytic Hydrogen Production

Yan Chen , Xiuli Fu , Zhijian Peng *

Posted Date: 19 May 2023

doi: 10.20944/preprints202305.1388.v1

Keywords: TiO2 crystals; Oxygen defects; Photocatalysis; Water splitting; Hydrogen production

Review

A Review on Oxygen-Deficient Titanium Oxide for Photocatalytic Hydrogen Production

Yan Chen [1,2], Xiuli Fu [2] and Zhijian Peng [1,*]

[1] School of Science, China University of Geosciences, Beijing 100083, China; 3019210003@cugb.edu.cn
[2] School of Science, Beijing University of Posts and Telecommunications, Beijing 100876, China; xiulifu@bupt.edu.cn
* Correspondence: pengzhijian@cugb.edu.cn; 86-10-82320255

Abstract: Photocatalytic technology based on specific band structure of semiconductors offers a promising way to solve the urgent energy and environmental issues in modern society. In particular, hydrogen production from water splitting over semiconductor photocatalysts attracts great attention owing to the clean source and application of energy, which highly depends on the performance of photocatalysts. Among the various photocatalysts, TiO_2 has been intensively investigated and used extensively due to its outstanding photocatalytic activity, high chemical stability, non-toxicity and low cost. However, pure TiO_2 has a wide band gap of approximately 3.2 eV, which limits its photocatalytic activity for water splitting to generate hydrogen only under ultraviolet light, excluding most of the inexhaustible sunlight for human beings. Fortunately, the band gap of semiconductors can be manipulated, in which introducing oxygen defects is one of the most effective measures to narrow the band gap of titanium oxides. This review starts out by the fundamentals of photocatalytic water splitting for hydrogen production over TiO_2, discusses the latest progress in this field, and summarizes the various methods and strategies to induce oxygen defects in TiO_2 crystals. Then, the next section outlines the modification approaches of oxygen-deficient titanium oxide ($TiO_{2-\delta}$) to further improve its photocatalytic performance. Finally, a brief summary and outlook of the researches on $TiO_{2-\delta}$ photocatalysts for water splitting to produce hydrogen were presented.

Keywords: TiO_2 crystals; oxygen defects; photocatalysis; water splitting; hydrogen production

1. Introduction

The exploitation and utilization of fossil fuels, such as coal, oil, and natural gas, facilitates the development of industrialization and urbanization. However, fossil fuels are non-renewable resources, whose reserves are limited, which will certainly become scare. In addition, the use of fossil fuels has dramatically induced negative effects on ecological environment. For instance, carbon dioxide emitted during fossil fuel burning is one of the main greenhouse gases. The industrial by-products and wastes cause severe pollution to the environment. Some pollutants even harm the human health by accumulating through food chain. Hence, it is necessary and urgent to develop sustainable energy to replace fossil fuels. Up to now, some renewable energy sources, such as solar energy, wind power and geothermal power, are being greatly developed and widely used in the world. However, the replacement of fossil fuels still remains elusive due to the restriction on technique and economy [1–6].

Among the many candidates, hydrogen energy is considered as one of the most promising energy carriers. Hydrogen is one of the most abundant elements on earth, and hydrogen energy can be obtained from a variety of natural resources. Moreover, hydrogen has superb combustibility, high ignition point (585 °C) and high heat of combustion (1.42×10^5 kJ·kg^{-1}). Compared with most of the common fuels, it has unparalleled superiority (see Table 1). Additionally, the combustion product of hydrogen contains only water (Equation 1), while the burning of fossil fuels will produce a large

Preprints (www.preprints.org) | NOT PEER-REVIEWED | Posted: 19 May 2023 doi:10.20944/preprints202305.1388.v1

quantity of carbon dioxide, sulfur oxide, nitrogen oxide and so on, which are associated with a series of severe environmental issues, including greenhouse effect, photochemical smog and acid rain [1,7–9]. Comparatively, hydrogen is certainly a clean, efficient and sustainable energy source with tremendous prospects for development. Nowadays, more than 95% of hydrogen in industry is produced from fossil energy, such as natural gas, petroleum and coal. However, these traditional processes for hydrogen production emit a large amount of exhaust gases like carbon dioxide, which weakens the advantage of using hydrogen as clean energy. And low efficiency and subsequent purification of the resultant hydrogen in these processes are also of great challenge [10–13]. Besides, producing hydrogen by water electrolysis is also an important method to prepare hydrogen in large scale, but it will consume a large amount of electric energy [14,15]. Fortunately, in 1972, Fujishima and Honda reported the decomposition of water to produce hydrogen over a TiO_2 electrode under ultraviolet light irradiation, thus initiating a new age of catalysis [16]. The emergence of photocatalytic technology provides a new option for hydrogen production: producing hydrogen by photocatalytic water splitting. On the one hand, there are abundant resources of raw material because over 70% of the surface of the Earth is covered by water. And the raw material water can be recycled in an ideal situation. On the other hand, the irradiation of photocatalytic reactions can be provided by sunlight, which is an inexhaustible resource for human beings. But the solar energy is an intermittent energy resource, so transforming solar energy into hydrogen is also beneficial to its effective storage and use [17–19].

Table 1. Heat of combustion and ignition point of some commonly used fuels.

Fuels	Heat of Combustion ($kJ \cdot mol^{-1}$)	Heat of Combustion ($kJ \cdot kg^{-1}$)	Ignition Point (℃)
hydrogen	285.8	1.42×10^5	585
coal	--	8.36×10^3 ~ 3.06×10^4	300 ~ 700
gasoline	--	4.31×10^4	427
diesel	--	4.26×10^4	220
kerosene	--	4.31×10^4	80
natural gas	--	3.89×10^4 $kJ \cdot m^{-3}$	650
wood	--	1.2×10^4	200 ~ 290
ethanol	1366.8	2.97×10^4	12
methane	890.3	5.55×10^4	538
butane	2653	4.56×10^4	365
acetone	1788.7	3.08×10^4	465
graphite	393.7	3.28×10^4	~ 650

$$H_2\,(g) + \frac{1}{2}O_2\,(g) = H_2O\,(l) \qquad H = -285.8\ kJ \cdot mol^{-1} \tag{1}$$

Photocatalyst is the key for producing hydrogen efficiently from the photolysis of water. In literature, TiO_2 was the first reported photocatalyst, which has been studied extensively and already applied in some specific area due to its high photocatalytic activity, non-toxicity, good stability, low cost and so on. Especially since 1990s, TiO_2 photocatalyst has made great progress in the fields of photodegradation of environmental pollutants and photocatalytic water splitting to produce hydrogen [20–22]. However, the utilization rate on solar energy by TiO_2 photocatalyst is very low due to the fact that TiO_2 could be excited only by short-wavelength ultraviolet light, which accounts for only about 5% of solar light. Consequently, scientists have paid great attention to develop the second-generation semiconductor photocatalysts of highly efficient visible-light-driven activity, including the modified TiO_2 photocatalysts and other non-TiO_2 photocatalysts.

Among the many already known methods, the construction of oxygen defects has been considered as one of most efficient ways to manipulate the band gap of titanium oxides. Literature survey indicates that oxygen-deficient titanium oxide ($TiO_{2-\delta}$) can absorb more visible light than stoichiometric TiO_2 [23–25]. The relevant experimental studies and theoretical calculations revealed

 doi:10.20944/preprints202305.1388.v1

that the new intermediate energy level associated with oxygen defects could reduce the band gap of TiO_2, which would thus lead to strong absorption of visible light, and the formation of oxygen defects in titanium oxide could also enhance its electrical conductivity, thus facilitating the transfer of photogenerated electrons [23,24]. As a result, many $TiO_{2-\delta}$ based photocatalysts with superb performance have been developed to generate hydrogen from water splitting [26,27]. Moreover, the band gap of TiO_2 can also be effectively adjusted by some other strategies, such as ion doping and compositing with narrow band gap semiconductors, in which the former one might be also concerned with the formation of oxygen defects. However, the fast recombination of photogenerated electrons (e_{CB}^-) and holes (h_{VB}^+) is also a key factor that results in low quantum efficiency of titanium oxide photocatalysts. Hence, other approaches including but not limited to ion doping, deposition of noble metals, and loading on supports are often adopted to enhance the photocatalytic activity of TiO_2 jointly with introducing oxygen defects [28–34].

Therefore, in this review, the mechanism of photocatalytic hydrogen production by water splitting over TiO_2 is firstly discussed in detail. Then the effect of introducing oxygen defects on the photocatalytic activity of TiO_2 is analyzed. And the last part of this section provides a brief overview of the research progress in photocatalytic water splitting to generate hydrogen over $TiO_{2-\delta}$ based photocatalysts. Afterwards, in Section II, a variety of methods to introduce oxygen defects into TiO_2 are summarized, and their merits and shortcomings are analyzed. This is of great guidance to select the proper techniques to develop $TiO_{2-\delta}$ based materials. In the following Section III, we will discuss the modification methods of TiO_2 photocatalysts in addition to the introducing oxygen defects, such as ion doping, deposition of noble metals, dye sensitization and so on, which are helpful for further enhancing the photocatalytic activity of $TiO_{2-\delta}$. Finally, the perspectives and existing challenges of photocatalytic water splitting into hydrogen over $TiO_{2-\delta}$ based photocatalysts are presented in the short section of Conclusions and Outlooks.

2. Fundamentals of Producing H_2 by Photocatalytic Water Splitting over TiO_2

2.1. Mechanism of Photocatalytic Water Splitting to Generate H_2

Photocatalysis technology is based on the special energy band structure of semiconductors. In ground state, the valence band (VB) of a semiconductor is fully occupied by electrons and the conduction band (CB) is empty. There is a quantized and discontinuous band gap between the low energy VB and high energy CB. And the band gap energy (E_g) of semiconductors is narrower than that of insulators (>5 eV). Therefore, the electrons in VB of a semiconductor can be excited and leap into CB when it was stimulated by photons with certain energy (higher than E_g), leaving the same number of holes in VB (Figure 1). Photogenerated e_{CB}^- and h_{VB}^+ possess strong reducing and oxidizing ability, respectively, and will migrate quickly to the surface of photocatalysts to participate in redox reaction [35]. The photocatalysts can directly decompose water when they are suspending in water, which does not require complex reaction system. Photocatalytic water splitting over semiconductors generally comprises the following five steps. (i) Water molecules are adsorbed on the surface of a photocatalyst. (ii) The electrons in VB leap into CB, producing e_{CB}^- and h_{VB}^+ under the irradiation by light. (iii) The photogenerated e_{CB}^- and h_{VB}^+ transfer to the surface of the photocatalyst. (iv) The e_{CB}^- reduces H^+ into hydrogen and h_{VB}^+ oxidizes H_2O to oxygen, which are commonly referred as hydrogen evolution reaction and oxygen evolution reaction. (v) The produced hydrogen and oxygen were desorbed from the surface of the photocatalyst. Among them, steps II-IV are the rate-determining steps on the photocatalytic water splitting (see Equations 2-5).

Preprints (www.preprints.org) | NOT PEER-REVIEWED | Posted: 19 May 2023 doi:10.20944/preprints202305.1388.v1

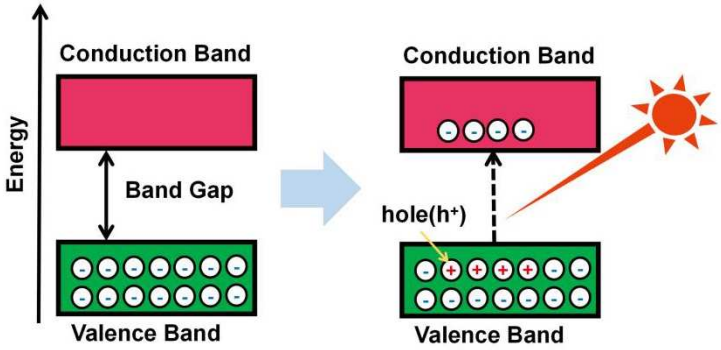

Figure 1. Schematic illustration of the energy band structure of semiconductors.

$$SC + 2hv \rightarrow 2e^- + 2h^+ \quad (2)$$

$$2H^+ + 2e^- \rightarrow H_2 \quad (3)$$

$$2H_2O + 2h^+ \rightarrow O_2 + 2H^+ \quad (4)$$

$$\text{Overall reaction: } H_2O + 2hv \rightarrow H_2\,(g) + O_2\,(g) \quad (5)$$

During photocatalytic water splitting, firstly, only the photons carrying energy greater than the E_g value of a semiconductor can excite the valance electrons into CB. Because the E_g value of TiO_2 is about 3.2 eV, so only the ultraviolet light with wavelength less than 380 nm can excite its valance electrons. Next, apart from moving to the surface of the semiconductor to participate in redox reaction, those excited electrons will also recombine with the holes, releasing light and/or heat energy. The recombination of e_{CB^-} and h_{VB^+} is the deactivation process of the photogenerated carriers, which does not contribute to the photocatalytic water splitting, and should be avoided as much as possible (Figure 2a) [36]. Moreover, the reducing ability of e_{CB^-} depends on bottom of CB (CB minimum) and the oxidizing ability of h_{VB^+} relies on top of VB (VB maximum). The necessary conditions for photocatalytic water splitting are that the CB minimum is more negative than the reduction potential of H^+/H_2 (0 V vs. NHE at pH=0) and the VB maximum is more positive than the oxidation potential of H_2O/O_2 (1.23 V vs. NHE at pH=0). This requires an E_g value no less than 1.23 eV, covering the oxidation-reduction potential of H_2O. In fact, the E_g value of photocatalysts for photocatalytic water splitting is generally required more than 1.9 eV due to the influence of mechanical and thermodynamic losses. Specifically, the CB minimum and VB maximum of TiO_2 are about -0.2 and 3 eV, respectively. Therefore, TiO_2 can split water into hydrogen and oxygen efficiently through photocatalysis (Figure 2b) [37].

Preprints (www.preprints.org) | NOT PEER-REVIEWED | Posted: 19 May 2023 doi:10.20944/preprints202305.1388.v1

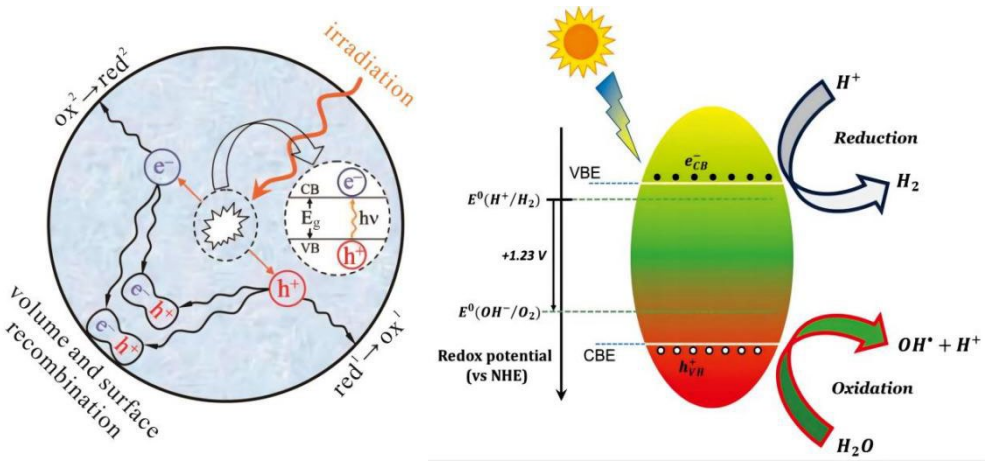

(**a**) (**b**)

Figure 2. (**a**) Behavior of photogenerated carriers in a semiconductor [36]. (**b**) Schematic illustration of the mechanism during photocatalytic water splitting over a semiconductor [37].

2.2. Impact of Oxygen Defects on the Photocatalytic Activity of TiO_2

As mentioned above, TiO_2 can only absorb ultraviolet light because of its wide band gap. However, a large proportion (about 50%) of the solar spectrum is visible light. Thus, enhancing the capability of harvesting visible light is an effective way to improve the photocatalytic performance of TiO_2. In literature, it was reported that the original white TiO_2 would be turned black after it was thermally treated with H_2, indicating that the light absorption capability of the reduced TiO_2 (actually $TiO_{2-\delta}$) was significantly enhanced. Moreover, it has been proved that the light absorption spectrum edge of $TiO_{2-\delta}$ will shift to long wavelength as the density of oxygen defects increased (Figure 3a), and the corresponding E_g decreased (Figure 3b) [23,38,39]. When there is an oxygen vacancy, one atom of oxygen in TiO_2 is bonded with three Ti atoms and two redundant electrons are shared by the surrounding three Ti atoms (see Figure 4a). A portion of Ti^{4+} will be converted into Ti^{3+} after trapping the redundant electrons. And the appearance of Ti^{3+} species in the nonstoichiometric $TiO_{2-\delta}$ is generally considered as the main reason that causes its absorption to visible light. Ti^{3+} species caused by oxygen defects can introduce new intermediate defect states (shallow donor) below the bottom of CB and modify the band gap structure of TiO_2 (Figure 4b–d), which means that $TiO_{2-\delta}$ has a narrower band gap and thus can absorb visible light [23,25,40,41].

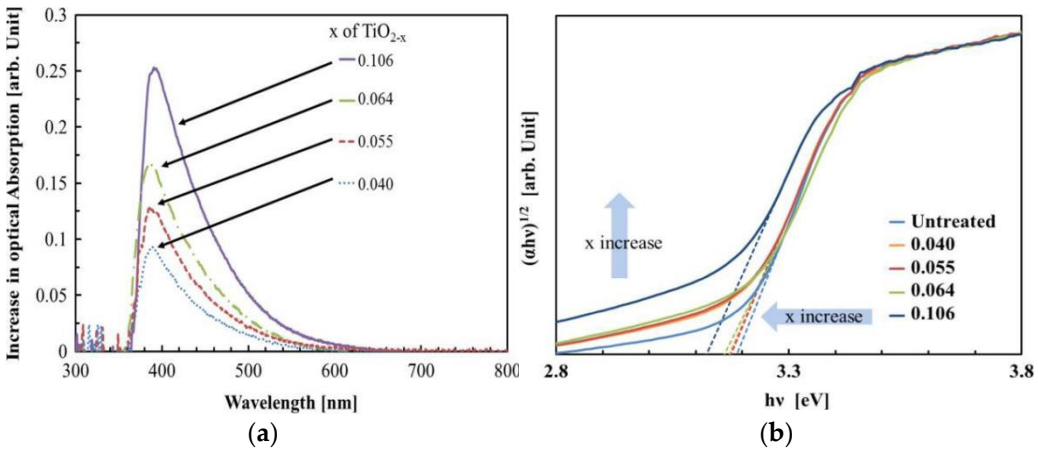

(**a**) (**b**)

Figure 3. (**a**) Optical absorption of various TiO_{2-x} samples and (**b**) their corresponding band gaps [38].

On the other hand, the presence of oxygen vacancies enlarges the lattice spaces of TiO_2. Resultantly, the resistance for electron transfer will decrease. A low resistance for electron transfer is

Preprints (www.preprints.org) | NOT PEER-REVIEWED | Posted: 19 May 2023 doi:10.20944/preprints202305.1388.v1

beneficial to the quick transfer of photogenerated electrons, thus suppressing the recombination of photogenerated e_{CB}^- and h_{VB}^+ [42]. For example, Hao *et al*. [43] prepared an oxygen-deficient blue titanium oxide, reporting that the prepared $TiO_{2-\delta}$ electrode would present a much lower charge transfer resistance (87 Ω) compared with its TiO_2 counterpart (356 Ω) (Figure 4e,f) [43]. Additionally, the bridging oxygen vacancies are tended to cause the Ti 3d defect state in the band gap of TiO_2. The Ti interstitials in the near-surface region can provide the electronic charges that the photocatalytic reactions need [44]. As a result, $TiO_{2-\delta}$ will present a higher photocatalytic performance than TiO_2.

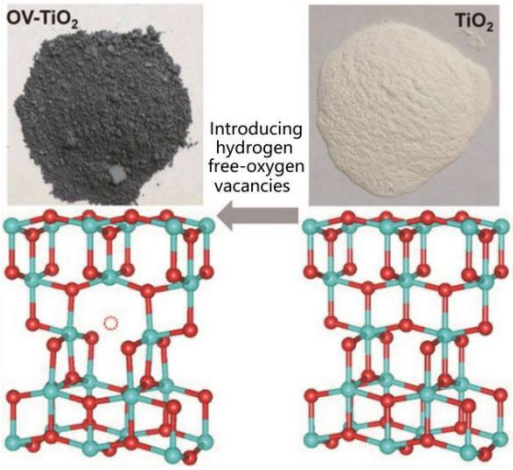

(a)

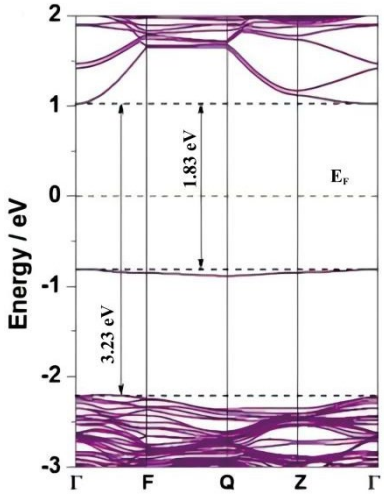

(b)

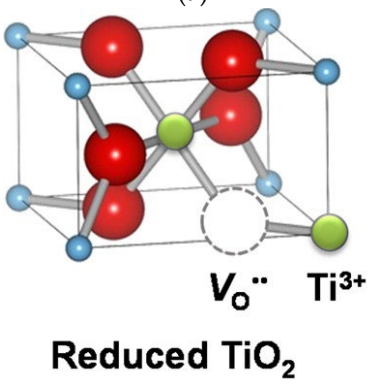

(c)

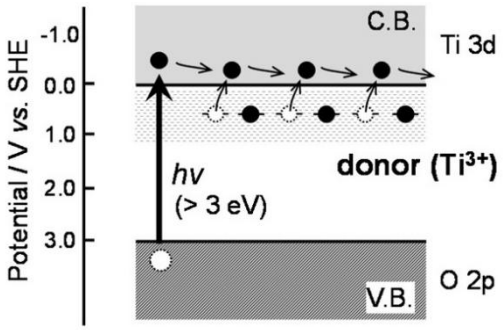

(d)

(e)

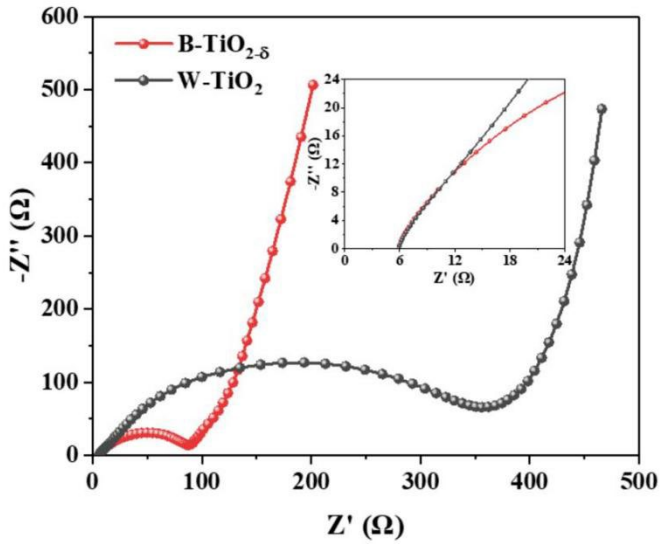

(f)

 doi:10.20944/preprints202305.1388.v1

Figure 4. (**a**) Digital images for the atomic structures of anatase TiO_2 and oxygen-deficient TiO_2 (blue and red balls indicate titanium and oxygen atoms, respectively) [23]. (**b**) The calculated band structures of oxygen deficient TiO_2 [23]. (**c**,**d**) Illustrations on oxygen vacancy and donor states owing to Ti^{3+} [40]. (**e**,**f**) Photographs and Nyquist plots at room temperature of black $TiO_{2-\delta}$ and white TiO_2. The inset shows the enlarged view of the semicircle regions and the equivalent circuit in the high-frequency region [43].

2.3. Brief Overview on Photocatalytic Water Splitting to Generate H_2 over $TiO_{2-\delta}$

Since the earliest report on light-driven water splitting by Fujishima and Honda in 1972 [16], semiconductor photocatalysis has attracted great attention in the field catalysis. However, for a quite long period, semiconductor photocatalysis developed in a mild speed and many researches were focused on the photodegradation of pollutants [45–48]. After entering 21st century, the researches on semiconductor photocatalysis have grown explosively and quite a lot of photocatalysts with excellent performance have been developed [21,29,36]. In particular, although oxygen vacancy was reported to generate a defect state in the band gap of TiO_2, leading to a narrower band gap of $TiO_{2-\delta}$ in 1980s, $TiO_{2-\delta}$ based photocatalysts are promptly developed and applied to water splitting until recent ten years [32,49].

In 2008, Sasikala *et al.* [50] synthesized a series of Sn- and Eu-doped TiO_2 ($Ti_{1-(x+0.001)}Eu_{0.001}Sn_xO_{2-\delta}$, where $0.05<x<0.3$) nanoparticles, which showed an onset of light absorption at about 450 nm and high activity for hydrogen generation. Liu *et al.* [32] subsequently reported an oxygen-deficient anatase TiO_2 nanosheet with dominant (001) crystalline plane, indicating that a special electron-transfer process on the reconstructed surface of TiO_2 substantially enhanced the hydrogen evolution rate from photocatalytic water splitting. TiO_2 treated by H_2 at high temperature also presented an enhanced photocatalytic activity for water oxidation and high apparent quantum efficiency for O_2 evolution (41% under light irradiation at 365 nm) [51]. An electron beam irradiated titania film shows wider range of absorbed light and higher efficiency of hydrogen production owing to the oxygen vacancies or defects enhancing mobility and separation of electrons and holes [52]. Other oxygen-deficient TiO_2 samples obtained by using the Ion Layer Gas Reaction (Spray-ILGAR) technique, microwave induced reduction, and solution plasma process also show high photocatalytic hydrogen evolution activity [53,54]. In summary, many $TiO_{2-\delta}$ based photocatalysts have been developed, but most of them are used to degrade pollutants and only a limited number of them are used to split water [24,26,27,31,35,55–58]. Among these limited reports, thermal treatment in hydrogen is the most widely used method of introducing oxygen defects in TiO_2 [24]. And the introduced oxygen defects in TiO_2 are generally combined with other strategies like ion doping and composing with other semiconductors to achieve high hydrogen evolution activity, which are also the recent researches that focus on [59–66].

3. Methods of Introducing Oxygen Defects in TiO_2

3.1. Reductive Treatment

Reductive treatment is the most direct way to introduce oxygen defects in TiO_2. TiO_2 can be reduced into $TiO_{2-\delta}$ by adding proper reducing agent. Among the many reductants, H_2 is the most widely used option because of its strong reducing ability and no impurities introduced [24,33,67–69]. However, H_2 treatment is usually carried out at high temperature and the explosion limit of H_2 falls in a very wide range of 4.0~75.6 vol.%. In other word, the operation of H_2 treatment on TiO_2 is quite dangerous, which needs very accurate processes. Moreover, treating TiO_2 with H_2 is usually a time-consuming work. For example, Xu *et al.* [70] reported black TiO_2 through H_2 treatment in a 20.0 bar of H_2 atmosphere at about 200 °C for 5 days. Zhang *et al.* [71] prepared defective $TiO_{2-\delta}$ hollow microspheres also by high-temperature H_2 reduction for 3 h at 550 °C. Wierzbicka *et al.* [72] synthesized a reduced "grey" brookite TiO_2 photocatalyst by hydrogenating at 500 °C, showing a remarkable noble metal free photocatalytic H_2 evolution performance, substantially higher than that of hydrogenated anatase or rutile TiO_2. The density of defects can be adjusted by tuning the H_2

Preprints (www.preprints.org) | NOT PEER-REVIEWED | Posted: 19 May 2023 doi:10.20944/preprints202305.1388.v1

treatment temperature, soaking time and H_2 concentration. For instance, Samsudin *et al.* [73] put TiO_2 into a continuous flow of 1 atm of pure H_2 at 500 °C for different times, finally obtaining $TiO_{2-\delta}$ with different densities of oxygen defects. They indicated that with time of H_2 treatment, the density of oxygen defects increased, the color of the products becomes deeper and deeper from white to dark gray and to bluish-gray (Figure 5a), and the light absorption ability of the resultant $TiO_{2-\delta}$ was significantly enhanced (Figure 5b). But more defects do not always guarantee better photocatalytic performance. Here, the photocatalytic of TiO_2 hydrogentreated for 24 h is inferior to that of the sample treated for 12 h. Thus, the control of oxygen defects density in TiO_2 is also important.

Apart from H_2, some other gases have been also used as the reductants. For example, NH_3 is also often used to reduce TiO_2. Chen *et al.* [56] synthesized a N-doped and oxygen-deficient TiO_2 photocatalyst by heating the commercially available pure TiO_2 in NH_3 atmosphere at 550 °C for 5 h. It is easy to introduce N into TiO_2 (N doping) when using NH_3 as the reducing agent. Similarly, Ihara *et al.* [74] prepared a N-doped oxygen-deficient titanium oxide by calcinating the hydrolytic product of $Ti(SO_4)_2$ with ammonia in dry air at 400 °C for 1 h. Additionally, some familiar reducing substances like carbon, $NaBH_4$ and Li can be also used to prepare oxygen-deficient TiO_2. Guan *et al.* [75] prepared a product of oxygen-deficient TiO_2 by a three-step process, which shows strong absorbance over the whole visible light region. In their process, a Ti coating was first pretreated in carbon powder at 1073 K for 2 h, which were then oxidized at 1073 K for 15 h in air. Next, the obtained samples were treated in carbon powder again at 973 K for 30 min, finally obtaining the product of oxygen-deficient TiO_2. Zhao *et al.* [76] first prepared TiO_2 anatase nanorods by a two-step hydrothermal method. Then, the obtained sample was mixed with $NaBH_4$ (1:1 in mole) in a mortar and thermally treated in Ar at 300 °C for 30 min, finally acquiring the reduced anatase nanorods. Interestingly, Martinze *et al.* [77] prepared a reduced blue TiO_2 by using Li foil and TiO_2 which were solved in ethylene diamine, stirring in anhydrous and dark conditions for 1440 h.

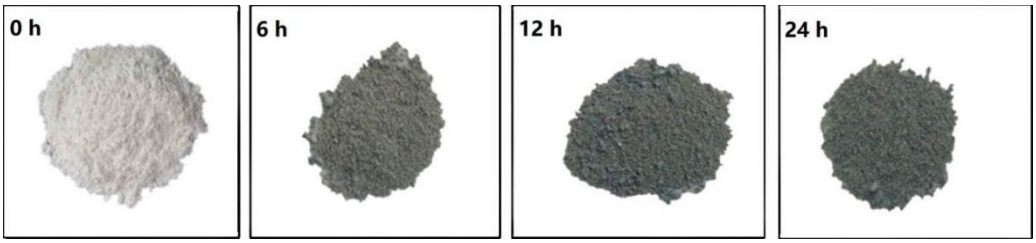

(**a**)

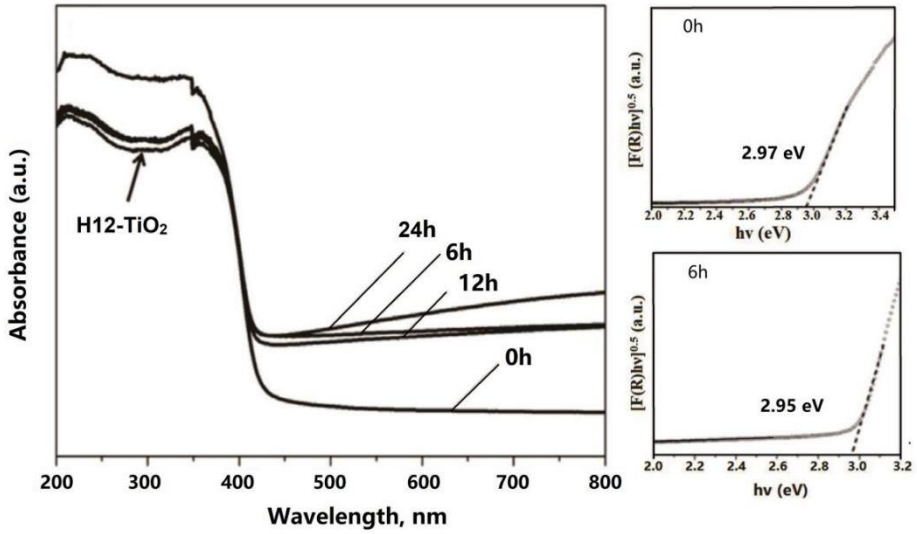

(**b**)

Figure 5. (**a**) digital images and (**b**) absorption spectra together with K-M functions showing the calculated band gap interpolation for TiO_2 hydrogenated for different times [73].

Preprints (www.preprints.org) | NOT PEER-REVIEWED | Posted: 19 May 2023 doi:10.20944/preprints202305.1388.v1

In addition, providing an anoxic environment in the treatment process of TiO_2 can also result in the same effect of adding reducing agents. For example, Pereira *et al.* [78] obtained oxygen-deficient TiO_2 films with enhanced visible and near-infrared optical absorption by periodically interrupting the O_2 gas supply in the process of magnetron sputtering. Dhumal *et al.* [79] synthesized oxygen-deficient titanium suboxide (TiO_x with $x<2$) nanoparticles by using a diffusion flame aerosol reactor under an oxygen lean environment in the formation zone of particles. Xiao *et al.* [80] reported the formation of oxygen vacancies in TiO_2 during the process of calcining TiO_2 in Ar or N_2 atmosphere. Kushwaha *et al.* [81] prepared a black oxygen-deficient TiO_2-graphite nanocomposite by calcining Ti-EDTA complex under hypoxic conditions. Singh *et al.* [41] investigated the effect of thermal treatment on TiO_2 thin films under an oxygen anoxic environment, reporting a reduction in band gap of 0.36 eV.

3.2. Pulsed Laser Irradiation

The excimer laser is a powerful tool and often used to manipulate the composition and structure of the material surfaces. Pulsed laser irradiation is a simple process for producing black oxygen-deficient TiO_2. A photochemical reduction reaction will take place during the pulsed laser absorption, thereby resulting in the evolution of oxygen deficiencies. The absorption of focused laser irradiation accompanied by fast heating cooling processes will promote the formation of porous surface [82]. As mentioned before, the dangers involved in hydrogenation operation greatly limit its application, while hydrogen plasma irradiation overcomes this shortcoming well [83,84]. For example, Wang *et al.* [83] synthesized a black titania with a core/shell structure (TiO_2@$TiO_{2-x}H_x$) assisted by hydrogen plasma and its photocatalytic activity for water splitting and cleaning pollutants is much better than that of TiO_2. In addition, Nd:YAG, ArF, KrF and XeCl excimer laser are also frequently used the assisted methods besides hydrogen plasma [85,86]. Nakajima *et al.* [86] indicated that the TiO_2 crystal surface would be successfully reduced through ArF, KrF and XeCl excimer laser irradiation, forming an oxygen-deficient $TiO_{2-\delta}$ layer with a thickness of 160 nm. Moreover, as shown in Figure 6a, the resistance of TiO_2 decreased after laser irradiation. Significant diffuse scattering around the (220) reflection for a wide range of Q_x (0.04~0.04) over the irradiated sample (Figure 6b) indicated a strong local lattice distortion near the surface of the sample.

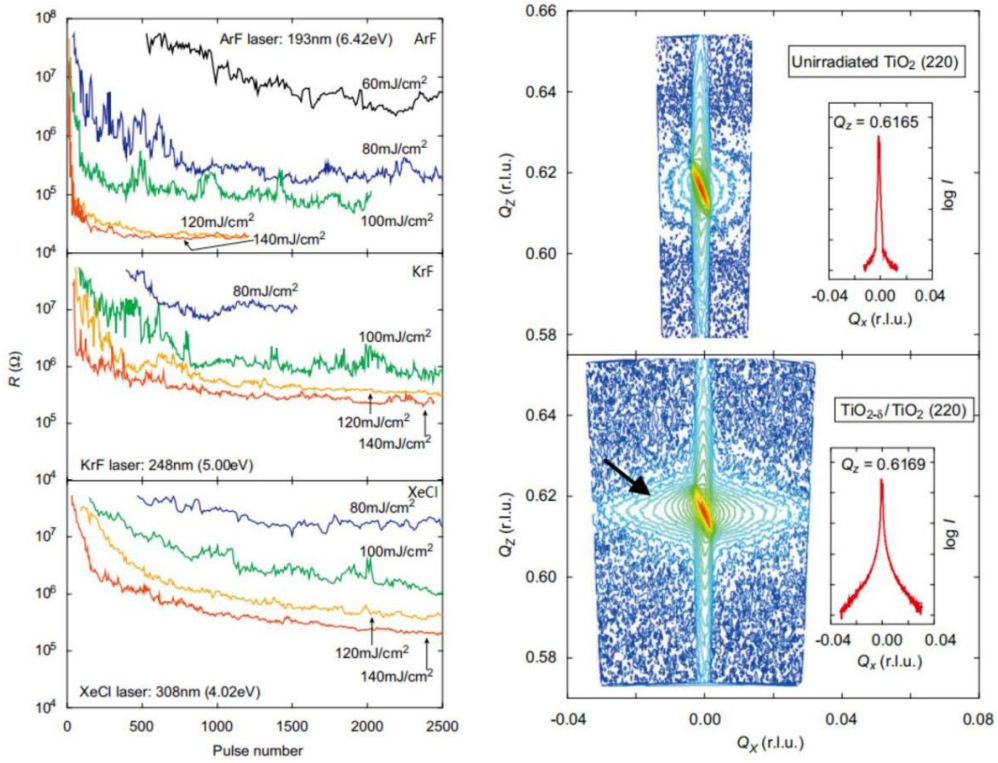

(**a**) (**b**)

Preprints (www.preprints.org) | NOT PEER-REVIEWED | Posted: 19 May 2023 doi:10.20944/preprints202305.1388.v1

Figure 6. (**a**) Surface resistance of TiO_2 (100) substrates as a function of pulse number irradiated by ArF, KrF and XeCl lasers. (**b**) Reciprocal space mappings around the (220) reflection for the unirradiated TiO_2 (100) substrate and laser-irradiated $TiO_{2-\delta}/TiO_2$ (100) substrate. The insets show the Q_x profiles at the (220) reflection [86].

3.3. Pulsed Laser Deposition

Pulsed laser deposition (PLD) is a good technique to prepare functional thin films by depositing the ablated substances on a substrate. The oxygen deficiency in the film can be adjusted by controlling the partial pressure of O_2 and laser power density. For instance, Leichtweiss *et al.* [57] prepared oxygen-deficient titanium oxide films with an average composition of $TiO_{1.6}$ by PLD at room temperature, which presented high efficiency for the water-splitting reaction. Kunti *et al.* [87] deposited TiO_2-SiO_2 composite films on amorphous quartz substrates at different partial pressures of O_2 by PLD technique, revealing the generation of oxygen defects and Ti^{3+} states in the films. Moreover, ion doped oxygen-deficient TiO_2 films can be obtained by changing the humidity of environment, atmosphere and ion implantation [88–90]. For instance, Socol *et al.* [90] fabricated N-doped crystalline TiO_2 thin films by PLD in N_2 or N_2-O_2 mixture. Nath *et al.* [91] synthesized $TiO_{1.5}$ nanoparticles by varying the focusing conditions of pulsed laser ablation. Rahman *et al.* [92] prepared TiO_2 nanostructures with different morphologies and incorporation of oxygen vacancy defects on a Si substrate by a single-step, catalyst-assisted PLD method (Figure 7). The morphology can be controlled by adjusting the deposition temperature and template.

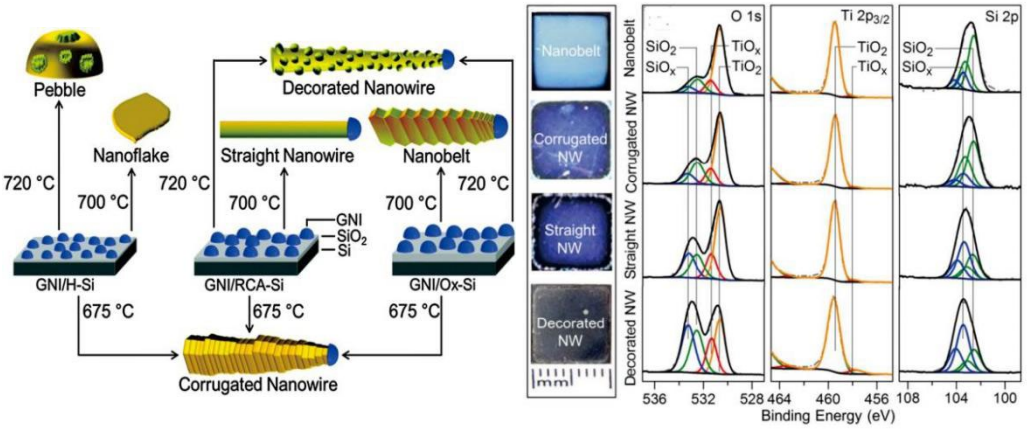

(**a**) (**b**)

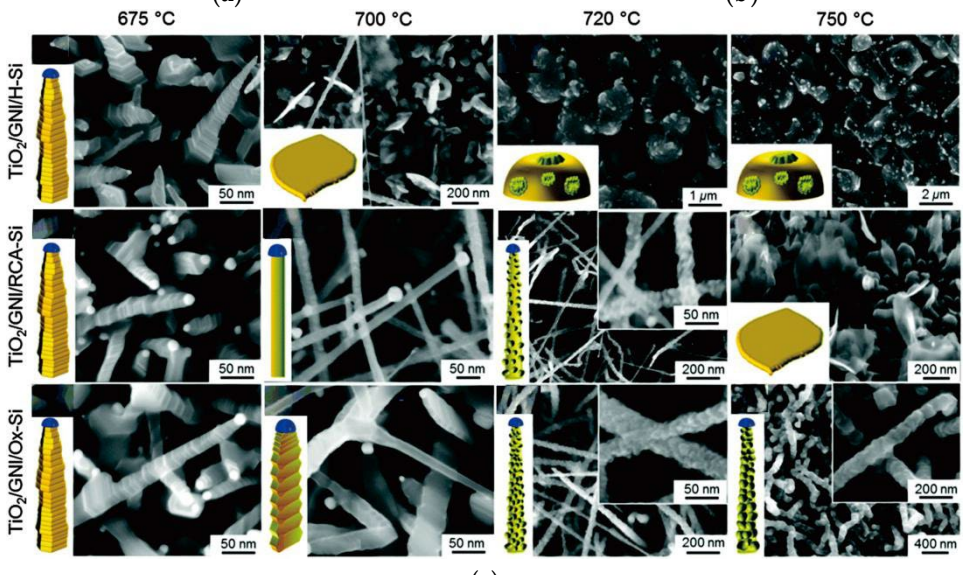

(**c**)

Preprints (www.preprints.org) | NOT PEER-REVIEWED | Posted: 19 May 2023 doi:10.20944/preprints202305.1388.v1

Figure 7. (**a**) Schematic models of TiO_2 nanostructures grown on gold nanoisland (GNI) modified Si (100) templates at 675, 700 and 720 °C. (**b**) Photographs and XPS spectra of O 1s, Ti 2p3/2, and Si 2p regions of TiO_2 films consisting of nanobelts, corrugated nanowires (NWs), straight NWs, and decorated NWs. (**c**) SEM images of TiO_2 nanostructures grown in 20 mTorr Ar at 675-750 °C on GNI modified H-terminated Si (GNI/H-Si), GNI modified RCA-cleaned Si (GNI/RCA-Si), and GNI modified thermally-oxidized (GNI/O_x-Si) templates. The corresponding lower left insets show schematic models of the as-grown nanostructures, and the upper right ones display the magnified SEM images of the selected nanostructures [92].

3.4. Ion Doping

Because of the difference in electronegativity between various elements, the introduction of impurity atoms into TiO_2 will change the partial concentration of electrons in TiO_2, thus producing oxygen defects in it. For instance, Ti^{4+} will be converted into Ti^{3+} when the oxygen atoms in TiO_2 are replaced by highly electronegative F atoms, due to the increased electron density around Ti^{4+} caused by the doped F atoms [93]. As shown in Figure 8a, clear Ti^{3+} signals can be observed in the EPR spectrum of fluorine-treated anatase. And the corresponding Raman spectra also display a slight shift to higher frequency at the peak of 144 cm^{-1}, which is attributed to the presence of oxygen vacancies and Ti^{3+} (Figure 8b). The oxygen vacancies are spontaneously introduced during N doping [94]. Pu *et al.* [95] successfully prepared N-doped oxygen-deficient TiO_2 microspheres through a two-step synthesis method. Firstly, TiO_2 microspheres are synthesized by solvothermal synthesis. Then, the final oxygen-deficient titanium oxide products were obtained by electron beam irradiation using urea as the nitrogen source, and the concentration of Ti^{3+} increased with increasing dose of the electron beam irradiation. Wang *et al.* [30] reported a N-doped TiO_2 ($TiO_{2-x}N_x$) by a simple wet method: hydrolyzing acidic tetra-butyl titanate in ammonia solution and following by calcination at 350 °C for 1 h. Of course, the nitrogen source for doping is generally directly or indirectly originating from reducing NH_3, which can also promote the reduction of TiO_2. Moreover, the doping of some metal ions, such as Eu^{3+}, $La^{3+}$and Gd^{3+}, can introduce oxygen defects in TiO_2 as well. Those ions with a lower valence than Ti^{4+} can generate anion vacancies in TiO_2 [96–98], thereby forming Ti^{3+} (Figure 8c). Zhang *et al.* [99] proved that the formation energy of a vacancy on the La-doped TiO_2 surface is lower than that formed on the pure TiO_2 surface treated in reducing conditions or oxidizing conditions by calculation (Figure 8d). Wang *et al.* [96] synthesized 0.4 mol% Gd and 2.0 mol% La co-doped TiO_2 microspheres via a hydrothermal method, which exhibit enhanced visible light absorption (Figure 8e). The doped La^{3+} and Gd^{3+} create abundant oxygen deficiencies and surface defects in the sample, decreasing the excitation energy of TiO_2 (Figure 8f).

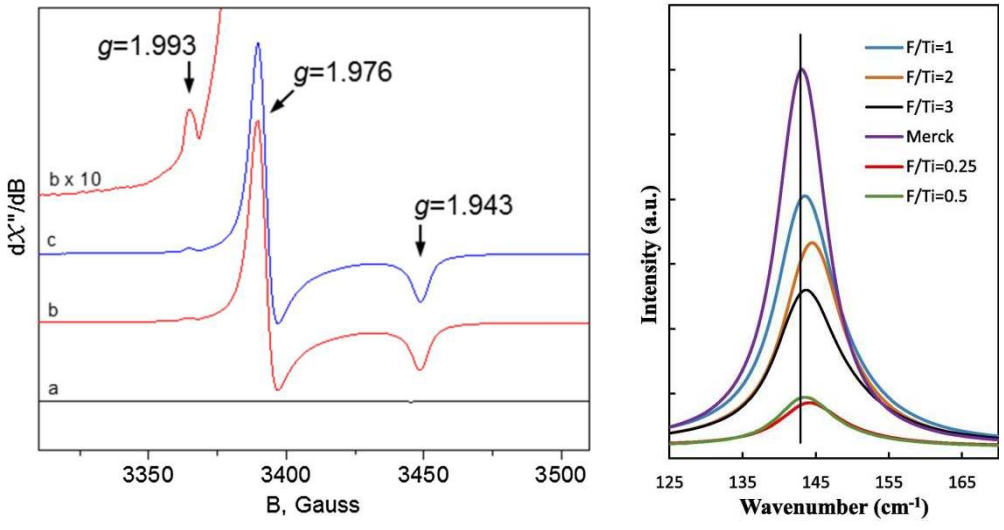

(**a**) (**b**)

Preprints (www.preprints.org) | NOT PEER-REVIEWED | Posted: 19 May 2023 doi:10.20944/preprints202305.1388.v1

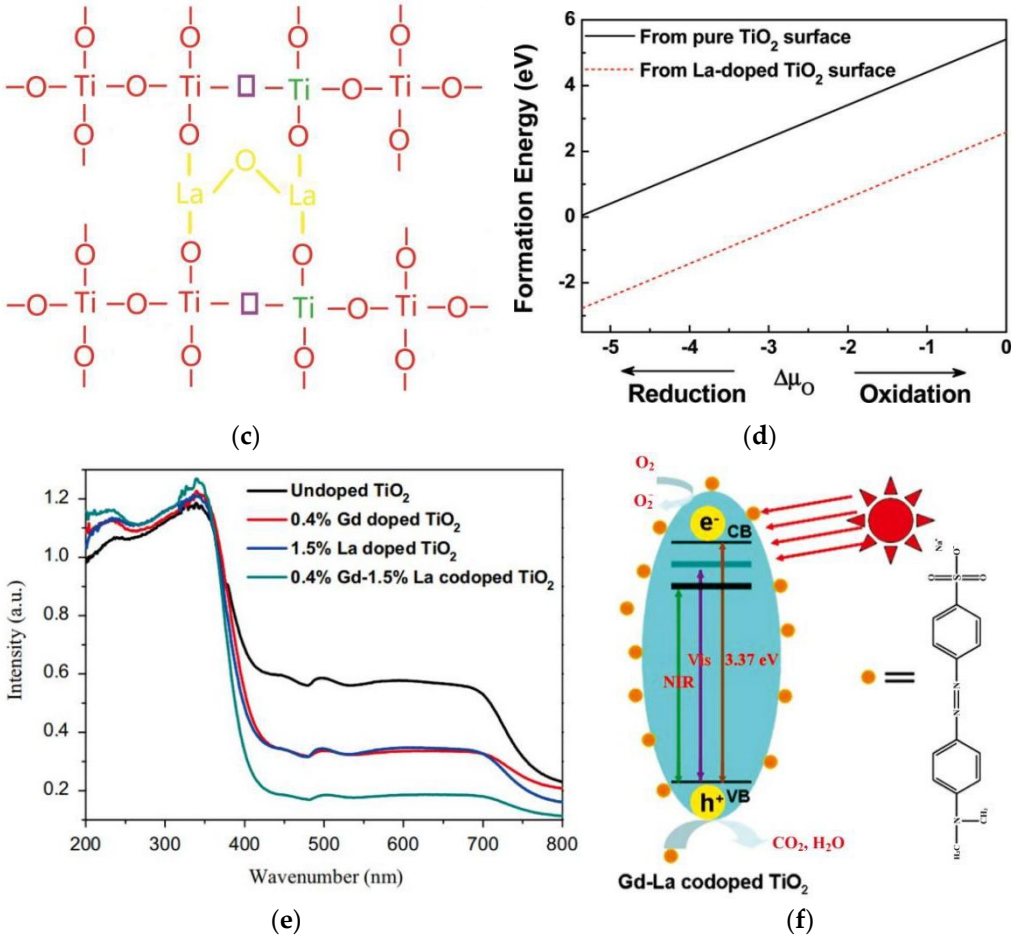

Figure 8. (**a**) EPR spectra and (**b**) Raman spectra of the anatase samples synthesized by a hydrothermal treatment with different HF amounts [93]. (**c**) Structural schematic of La doped TiO_2 [98]. (**d**) Formation energies of oxygen vacancies as a function of ΔμO (the difference in oxygen chemical potentials) [99]. (**e**) UV-vis diffuse reflection spectra of undoped, 1.5% La doped, 0.4% Gd doped, and 0.4% Gd-1.5% La co-doped TiO_2 nanoparticles [96]. (**f**) Schematic of the solar light induced photodegradation of methyl orange over the (Gd,La)-co-doped TiO_2 photocatalysts [96].

3.5. Plasma-Assisted Deposition

Plasma-enhanced chemical vapor deposition (PECVD) has the features of low deposition temperature, high purity, uniform thickness and composition of films, as well as easy control of reaction parameters. It can be used to prepare various metal films, inorganic films and organic films. The structure and properties of films can be adjusted by controlling reaction conditions. For example, Hatanaka *et al.* [100] prepared a-TiOx:OH films using a remote PECVD technique, which show high photoconductivity. Sakai *et al.* [101] obtained oxygen-deficient TiO_2 anatase films by using oxygen plasma assisted reactive evaporation by increasing the supply of titanium atoms, and the resultant oxygen deficient TiO_2 films showed excellent hydrophilicity, which was conducive to thoroughly contacting with water and facilitating its splitting reaction. Li *et al.* [102] introduced numerous oxygen deficiencies and Ti^{3+} defects on the surface of TiO_2 nanoparticles via Ar plasma (Figure 9a,b). Similarly, Hojo *et al.* [103] also successfully introduced oxygen defects in a TiO_2:Nb film by annealing the sample with Ar plasma irradiation. Recently, Kawakami *et al.* [104] reported a kind of anatase/rutile mixed phase TiO_2 nanoparticles with many oxygen deficiencies, which were obtained by annealing the sample with low-temperature O_2 plasma.

There are excited species like ozone and OH generated during the plasma discharge in water. Thus, plasma-liquid interaction has widely been applied to prepare nanomaterials. For instance, An *et al.* [105] prepared gray hydrogenated TiO_2 spheres by using a plasma modified sol-gel system. Mizukoshi *et al.* [106] obtained a blue TiO_2 containing oxygen defects by generating discharge plasma

Preprints (www.preprints.org) | NOT PEER-REVIEWED | Posted: 19 May 2023 doi:10.20944/preprints202305.1388.v1

in an aqueous ammonia solution containing TiO_2 powder. TiO_2 was reduced by the reducing species such as hydrogen radicals generated during the plasma discharge process in aqueous ammonia (Figure 9c–e).

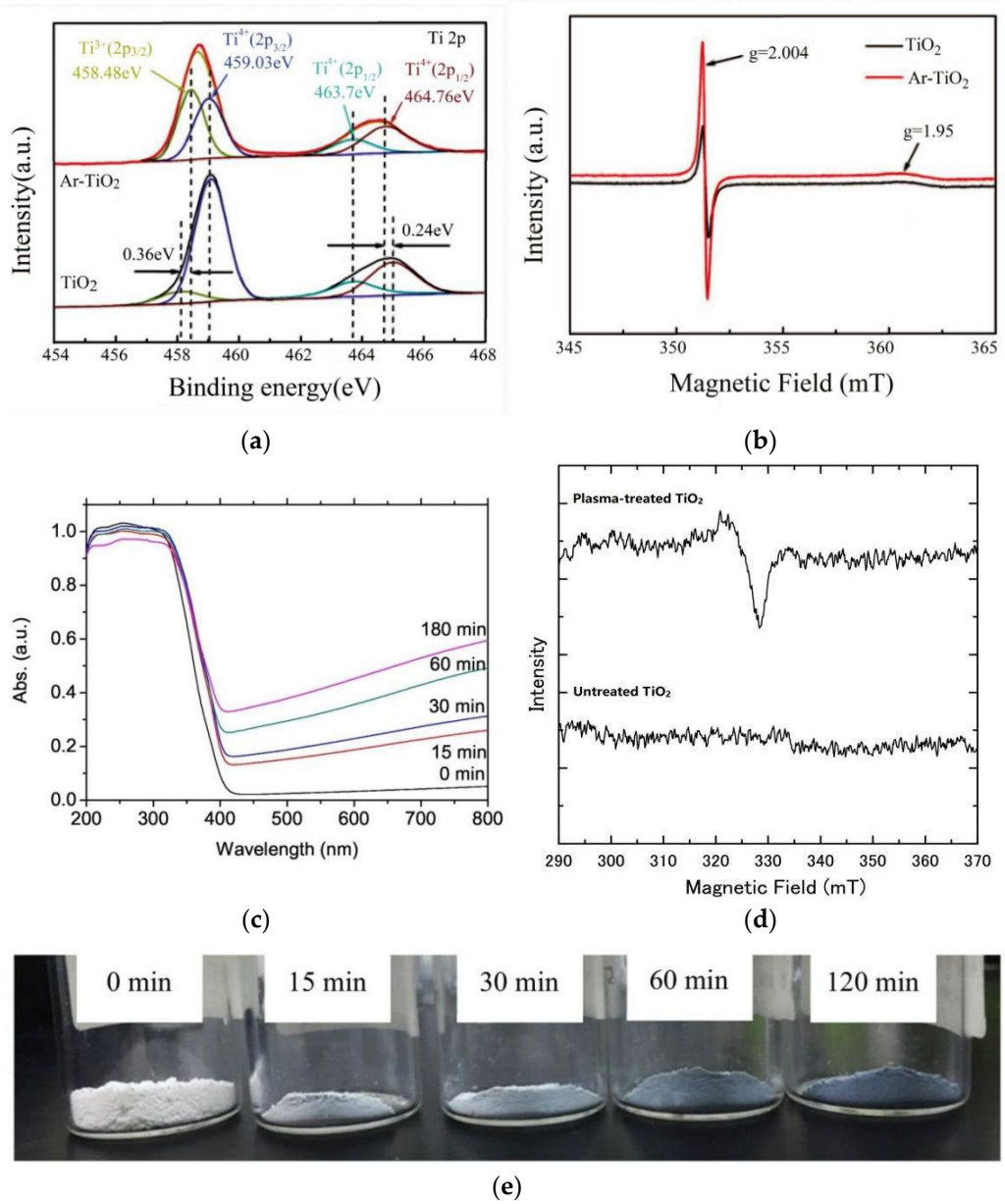

Figure 9. (**a**) Ti 2p XPS spectra of Ar plasma treated TiO_2 [102]. (**b**) EPR spectra for the Ar plasma treated and pristine TiO_2 [102]. (**c**) UV-vis spectra of TiO_2 after plasma treatment in aqueous ammonia solution for different times [106]. (**d**) EPR spectra of untreated and plasma-treated TiO_2 in aqueous ammonia solution [106]. (**e**) Digital photographs of TiO_2 after plasma treatment in aqueous ammonia solution for different times [106].

3.6. Ultrasonic Assisted Techniques

Ultrasonic spray pyrolysis is a simple, low-cost and scalable technique [107,108]. In literature, Nakaruk *et al.* [108] successfully prepared fully dense TiO_2 films with oxygen deficiencies by using ultrasonic spray pyrolysis and proved that the concentration of oxygen deficiencies could be controlled by changing the annealing temperature. Besides, oxygen vacancies can also be directly induced in TiO_2 by low-frequency ultrasound (LFUS) treating. For instance, Osorio-Vargas *et al.* [109] prepared visible-light responsive TiO_2-based photocatalysts by dispersing P25 powder into water and exposed to LFUS environment for 6 h. Bellardita *et al.* [110] reported that ultrasonic treating P25

Preprints (www.preprints.org) | NOT PEER-REVIEWED | Posted: 19 May 2023 doi:10.20944/preprints202305.1388.v1

powder dispersed in water induced oxygen deficiency in TiO_2 and thus narrowed the bandgap of TiO_2 from 3.18 to 3.04 eV.

3.7. Calcination under Anoxic Condition

Thermal treatment atmosphere exerts an important influence on the formation of oxygen deficiencies [111–114]. For instance, Albetran *et al.* [113] revealed that the color of titania changed from the white to gray and black as the ratio of Ar/air of thermal treating atmosphere increased (Figure 10a), and the light absorption of the corresponding products was also improved (Figure 10b). Sang *et al.* [114] fabricated oxygen-deficient TiO_2 nanotube arrays by calcining in nitrogen, or a mixture gas of 5% hydrogen in nitrogen (Figure 10c,d), which exhibit higher photocurrent density and smaller charge transfer resistance than that of the samples calcined in air (Figure 10e,f). Qi *et al.* [115] prepared a defective TiO_2 sample with oxygen deficiencies by thermally treating TiO_2 at 200 °C under vacuum conditions. The defect concentration in the sample is positively proportional to the thermal treatment time. Li *et al.* [116] reported an oxygen-deficient dumbbell-shaped anatase TiO_{2-x} product. In detail, a $TiCl_3$-HAc mixed solution was solvothermally treated at 180 °C for 5 h and the solvothermally synthesized product was calcined under vacuum at 400 °C for 1 h.

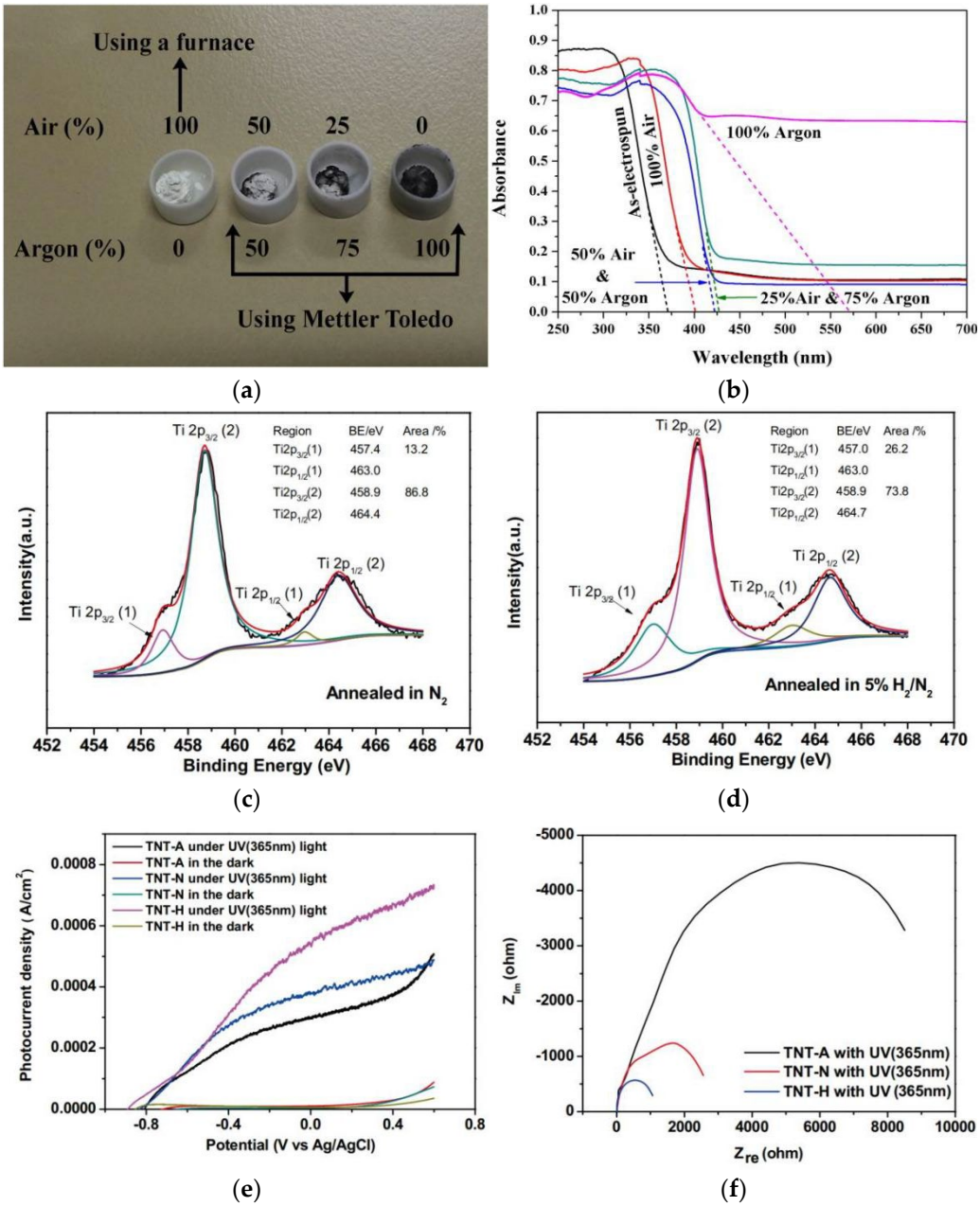

 doi:10.20944/preprints202305.1388.v1

Figure 10. (**a**) Digital photograph and (**b**) band gaps of the electrospun TiO_2 nanofibers prepared by non-isothermally heating from 25 to 900 °C at 10 °C/min in argon-air mixtures [113]. XPS spectra in Ti 2p region for anodized TiO_2 nanotubes annealed (**c**) in N_2 (TNT-N) and (**d**) in 5% H_2/N_2 (TNT-H) [114]. (**e**) Photocurrent density vs the applied potential of the TiO_2 nanotubes arrays annealed in air (TNT-A), N_2 (TNT-N) and 5% H_2/N_2 mixture gas (TNT-H) under ultraviolet light (365 ± 15 nm) irradiation and the control tests in the dark [114]. (**f**) Electrochemical impedance spectroscopy plots of the anodized TiO_2 nanotubes annealed in air (TNT-A), N_2 (TNT-N) and 5% H_2/N_2 mixture gas (TNT-H) under ultraviolet light illumination [114].

3.8. Molten Salt Calcination

Du *et al.* [117] reported a facile strategy based on molten salt calcination to construct oxygen deficiencies in TiO_2. A flower-like TiO_2 precursor was synthesized via solvothermal method using tetrabutyl titanate and acetic acid (HAc)/N,N-dimethyl formamide (DMF) as the titanium source and solvent, respectively. The as-prepared precursor was mixed with eutectic salts of LiCl/KCl (45/55 by weight) and calcined in a muffle furnace at 400 °C for 2 h. The lattice oxygen of TiO_2 was consumed during the calcination because of the low partial pressure of O_2 in the molten salt, thereby introducing numerous oxygen deficiencies and Ti^{3+} in the final product.

In summary, up to now, hydrogen reduction is still the most extensively used method to prepare oxygen-deficient TiO_2 owing to the strong deoxidizing ability and purity. But it is time-consuming and has to work under high temperature conditions. Thus, some other reductants like carbon, NH_3 and Li are also used to reduce TiO_2 in literature. Synthesizing titanium oxide in an anoxic environment is widely used as well because it is easily implemented. Pulsed laser irradiation is a simple process for producing oxygen-deficient TiO_2, which is, however, more suitable for treating films because the radiation response mainly happens in the surface layer. Similarly, oxygen-deficient TiO_2 films can be easily obtained through adjusting the partial pressure of O_2 and laser power density of PLD. Introducing oxygen defects through ion doping is a natural process and the density of oxygen defects mainly depends on the doped species of ions and their concentration. Plasma discharge in water will provide reductively excited species, which can easily reduce TiO_2. But it is currently not widely applied. Oxygen-deficient TiO_2 can be prepared by ultrasonic spray pyrolysis or calcinating under anoxic condition, and the density of oxygen deficiencies can be controlled by controlling the experimental temperature. Molten salt calcination is simple and easily operated.

4. Modification Methods of $TiO_{2-\delta}$ Photocatalysts

$TiO_{2-\delta}$ has been proved to perform better than stoichiometric TiO_2 in the process of photocatalytic water splitting. Many strategies such as ion doping, constructing heterojunction and deposition of noble metals can effectively improve the photocatalytic activity of TiO_2. Thus the photocatalytic activity of-$TiO_{2-\delta}$ should be enhanced further by these strategies.

4.1. Ion Doping

Ion doping can introduce defects into TiO_2, which could act as the capture traps of photogenerated carriers, thereby suppressing the recombination of photogenerated e_{CB^-} and h_{VB^+}. And the lattice distortion caused by the doped atoms with different ionic size would increase the asymmetry of crystal structure, which could promote the separation of photogenerated e_{CB^-} and h_{VB^+} as well. Additionally, the energy band structure of TiO_2 can be effectively manipulated by ion doping. The narrowed band gap can extend the light absorption and enhance the utilization efficiency on solar energy of the resultant photocatalysts.

4.1.1. Metal Ion Doping

The doping of transition metals has been proved an effective way for regulating the band positions of TiO_2. The main principle is to insert an additional energy level between the original conduction band and valence band. For example, Sheng *et al.* [118] reported a Pd doped TiO_2,

Preprints (www.preprints.org) | NOT PEER-REVIEWED | Posted: 19 May 2023 doi:10.20944/preprints202305.1388.v1

revealing that the photogenerated e_{CB}^- and h_{VB}^+ were efficiently separated after Pd doping. Sasirekha *et al.* [119] prepared a Ru doped anatase TiO_2 supported on silica by a solid-state dispersion method, which performed well in photocatalytic reduction of carbon dioxide. Gao *et al.* [120] indicated that the doping of Mo, Pd, Ru and Rh could narrow the band gap of TiO_2, thus enhancing the probability of activation by visible light. Their theoretically calculating results through density functional theory revealed that the impurity states of 4d electrons would form new degenerate energy levels, thus narrowing the band gap of TiO_2 (Figure 11). Thalgaspitiya *et al.* [121] synthesized mesoporous composites of M doped titanium dioxide (M = Mn, Co, Ni, Mo, and W) with reduced graphene oxide (rGO), indicating that the indirect band gap of the composites could be adjusted into the range of 2.20-2.48 eV.

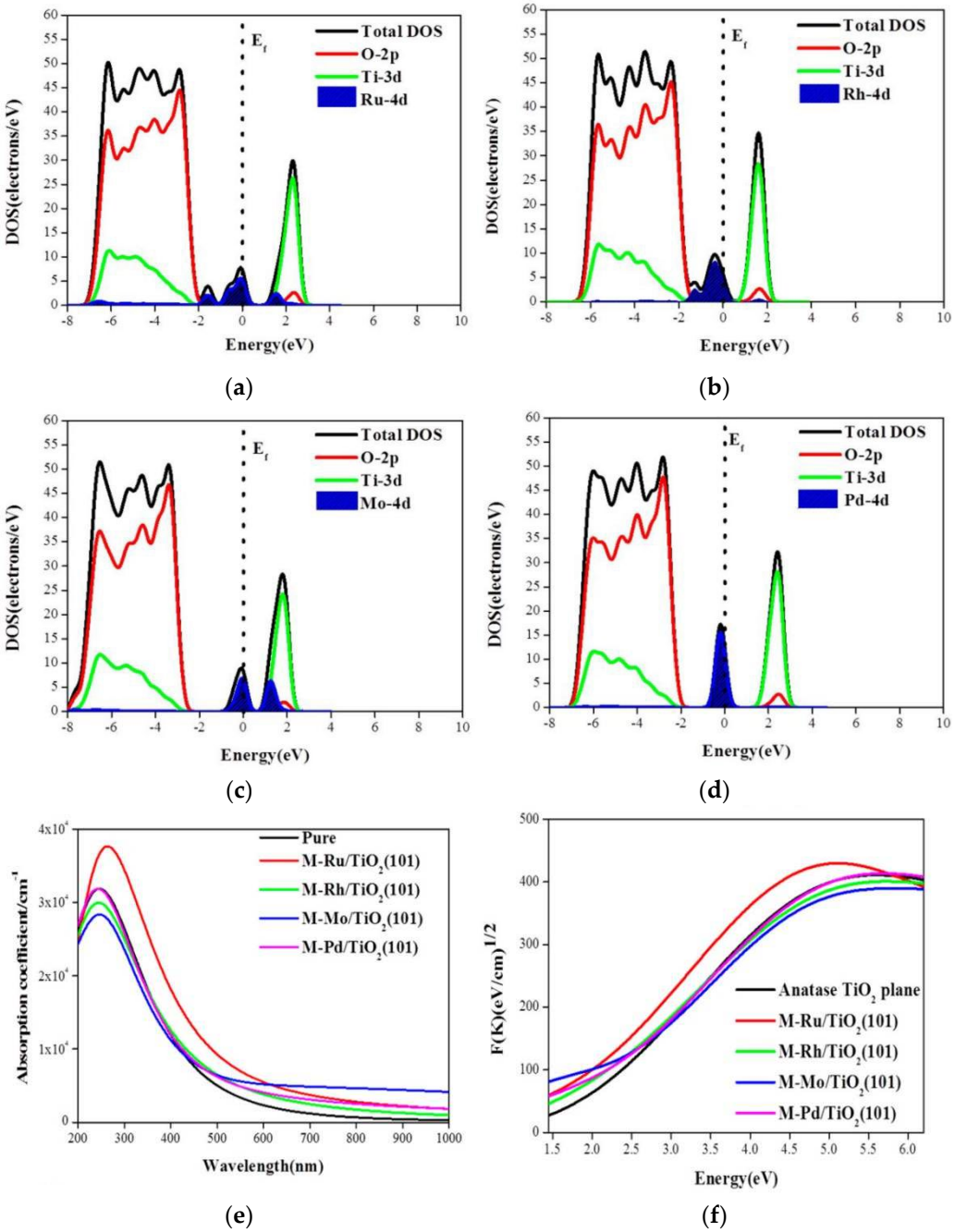

Figure 11. (**a**–**d**) Density of states, (**e**) optical absorption spectra and (**f**) Tauc plots of M doped (M = Pd, Ru, Mo, Rh) TiO_2 (101) with a monoatomic structure [120].

Preprints (www.preprints.org) | NOT PEER-REVIEWED | Posted: 19 May 2023 doi:10.20944/preprints202305.1388.v1

Rare earth ions have rich energy levels and unique features of 4f electronic transitions, providing unique opportunities for manipulating the band gap of semiconductors by elemental doping. For instance, Wang *et al.* [122] fabricated samples of La^{3+}- or Yb^{3+}-doped TiO_2 supported on r-GO, reporting that the anionic vacancies in TiO_2 lattice caused by La^{3+} and Yb^{3+} would generate Ti^{3+}, thus enhancing the visible-light response of the samples. Stengl *et al.* [123] prepared several samples of rare earth (La, Ce, Pr, Nd, Sm,, Eu, Dy, Gd) doped TiO_2, which are all visible-light sensitive. Fang *et al.* [124] synthesized rare earth ions (Er^{3+} and/or Yb^{3+}) doped TiO_2 photocatalysts by a hydrothermal method, indicating that the doping of Er^{3+} and/or Yb^{3+} could decrease the recombination rate of photogenerated electron-hole pairs, finally leading to the higher photocatalytic efficiency of TiO_2. In addition, the phase transition from anatase to rutile can be significantly delayed by the doping of rare earth ions [125,126].

Alkali metal and alkali earth metal ions were also used to improve the photocatalytic activity of TiO_2. Liu *et al.* [127] prepared a mesoporous Na doped titanium dioxide with a band gap of 3.08 eV. The doped Na ions could enter into the (004) crystalline plane of anatase TiO_2, finally leading to the dislocation defects in TiO_2. Lv *et al.* [128] successfully fabricated AM-TiO_{2-x} samples (AM = Mg, Ca, Sr, and Ba), revealing that the CB position of TiO_2 became more negative after AM-doping, thus improving the hydrogen production ability of TiO_2. Besides, the separation of carriers and transfer efficiency were also dramatically promoted (Figure 12a–c).

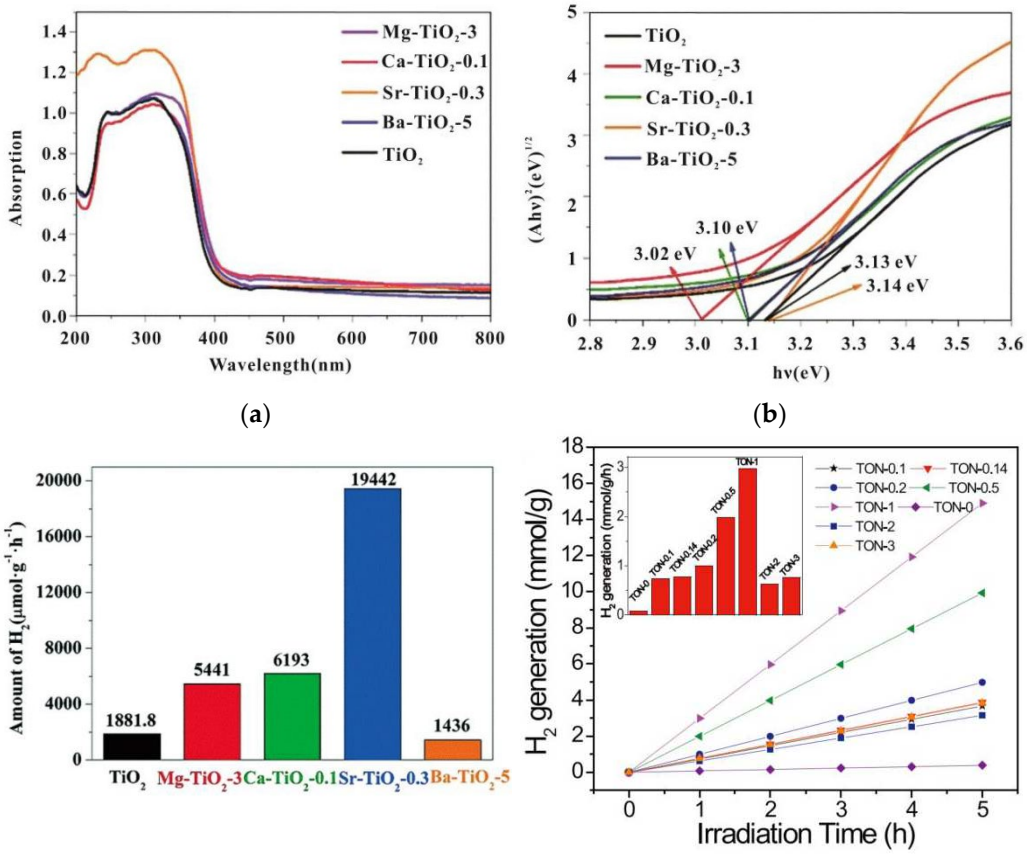

(**a**) (**b**)

(**c**) (**d**)

Preprints (www.preprints.org) | NOT PEER-REVIEWED | Posted: 19 May 2023 doi:10.20944/preprints202305.1388.v1

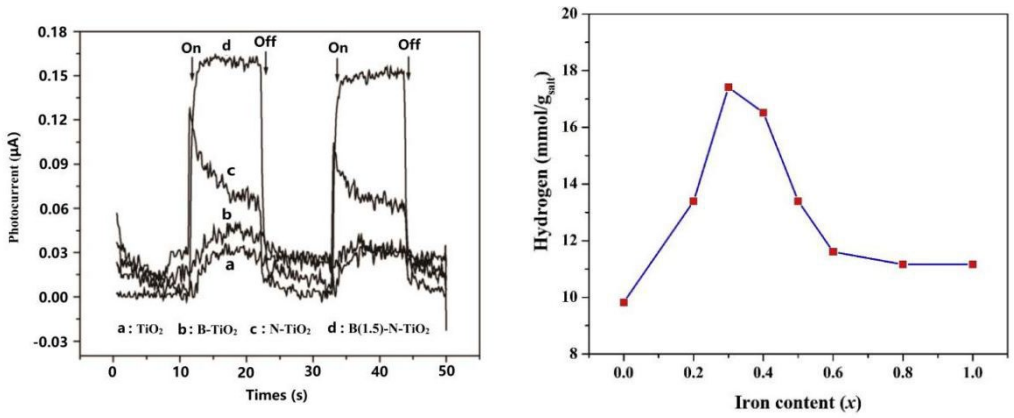

(**e**) (**f**)

Figure 12. (**a**) UV-vis diffuse reflectance spectra of TiO_2 and alkaline earth metal doped TiO_2 [128]. And (**b**) gaps of TiO_2 and alkaline earth metal doped TiO_2 [128]. (**c**) Photocatalytic H_2 production from water splitting over TiO_2 and alkaline earth metal doped TiO_2 under the condition of adding Pt as a co-catalyst [128]. (**d**) Photocatalytic H_2 generation over TiO_2 doped with different amounts of N [129]. (**e**) Photocurrent response curves of TiO_2, B-doped TiO_2, N-doped TiO_2 and (B,N)-co-doped TiO_2 to visible light [132]. (**f**) Photocatalytic H_2 generation over (Fe_xCo_{1-x})-co-doped TiO_2 [139].

4.1.2. Nonmetallic Ion Doping

The doping of nonmetallic ions can expand the light absorption region of TiO_2 and suppress the recombination of photogenerated e_{CB}^- and h_{VB}^+. Normally, the p orbital in the most outer electronic layer of the doped ions would hybridize with the 2p orbital of O in TiO_2, forming new shallow levels near the top of the valence band. For example, N doping is widely studied because the ion radius of N is closest to that of O [129–132]. Li *et al.* [129] prepared a N-doped TiO_2 which performs better in photocatalytic hydrogen evolution than undoped TiO_2 under the same conditions (Figure 12d). Yuan *et al.* [133] prepared a N-doped TiO_2 with high specific surface area by heating the mixture of urea and TiO_2. The absorption spectrum of the N-doped TiO_2 shifted to the wavelength up to 600 nm and the sample shows high photocatalytic activity on hydrogen evolution. Momeni *et al.* [134] prepared S-doped TiO_2 nanostructure photocatalyst films, which performed well in the removal of RhB and the hydrogen generation under visible light radiation. Carmichael *et al.* [135] reported B-doped titanium dioxide films with a hydrogen evolution rate of 24 μL cm^{-2} h^{-1}, which is far exceeded the undoped TiO_2 at 2.6 μL cm^{-2} h^{-1}. Wu *et al.* [136] fabricated F-doped TiO_2 particulate thin films, which could be applied in the photodegradation of organic pollutants and photoinduced splitting of water into hydrogen under the irradiation of either UV or visible light.

4.1.3. Multiple Ions Co-Doping

Different ions have different impacts on TiO_2 and thus the co-doping of multiple ions is an effective method to obtain higher photocatalytic activity. In literature, Zhu *et al.* [137] studied the electronic and optical properties of C-, Mo- and (Mo,C)-co-doped anatase TiO_2 using the first principles calculations. The results show that the optical absorption edges of the (Mo,C)-co-doped TiO_2 will shift towards the visible light region. Diao *et al.* [138] reported K, Na and Cl co-doped rutile TiO_2, exhibiting good photocatalytic degradation of gaseous formaldehyde under visible light irradiation. Li *et al.* [132] reported the photocatalytic activity for hydrogen production over (B,N)-co-doped TiO_2 under visible light irradiation. N doping extends the absorption edge to the visible light region and B doping acts as the shallow traps for photogenerated electrons to prolong the life of the electrons and holes. Consequently, stronger photocurrents were observed on (B,N)-co-doped TiO_2 than those on N-doped TiO_2, B-doped TiO_2 and undoped TiO_2 (Figure 12e). Barakat *et al.* [139] prepared Fe_xCo_{1-x}-co-doped titanium oxide nanotubes, achieving distinct enhancement on the visible light absorption capacity (Figure 12f). Filippatos *et al.* [140] even reported a photocatalyst of H, F and Cl co-doped titanium dioxide with high hydrogen production rate.

Preprints (www.preprints.org) | NOT PEER-REVIEWED | Posted: 19 May 2023 doi:10.20944/preprints202305.1388.v1

4.2. Composite

The heterostructure formed by the recombination of two or more semiconductors with matched energy band structure can effectively improve the separation efficiency of photogenerated e_{CB^-} and h_{VB^+}. The built-in electric field formed along the interface will promote the transfer of electrons (Figure 13) [141,142]. Additionally, the combination with narrow band semiconductor could allow TiO_2 to respond to visible light. For instance, Smith *et al.* [143] synthesized a nanotubular composite of TiO_2-WO_3. This composite demonstrated an increase of 46% in water splitting efficiency compared to TiO_2 nanotubes prepared under the similar conditions. Choudhury *et al.* [144] prepared ultra-thin PdO-TiO_2 composite films, which could be used to photogenerate hydrogen efficiently from a methanol-water for a long period of time. Navarrete *et al.* [145] synthesized β-Ga_2O_3/TiO_2 composite photocatalysts for H_2 production from a water/methanol mixture (Figure 14a). The high activity is attributed to slow charge recombination of the photogenerated e_{CB^-} and h_{VB^+} (Figure 14b). Gholami *et al.* [146] confirmed that the activity of ZnO-TiO_2 composite for photodegradation of bentazon is better than that over ZnO and TiO_2 separately. Chen *et al.* [147] constructed a NiO/TiO_2 heterojunction on the surface of TiO_2 film. The strong inner electrical field effectively separates the photogenerated electron-hole pairs, and thus the composite exhibited a much better photocatalytic activity than the original TiO_2 film (Figure 14c,d).

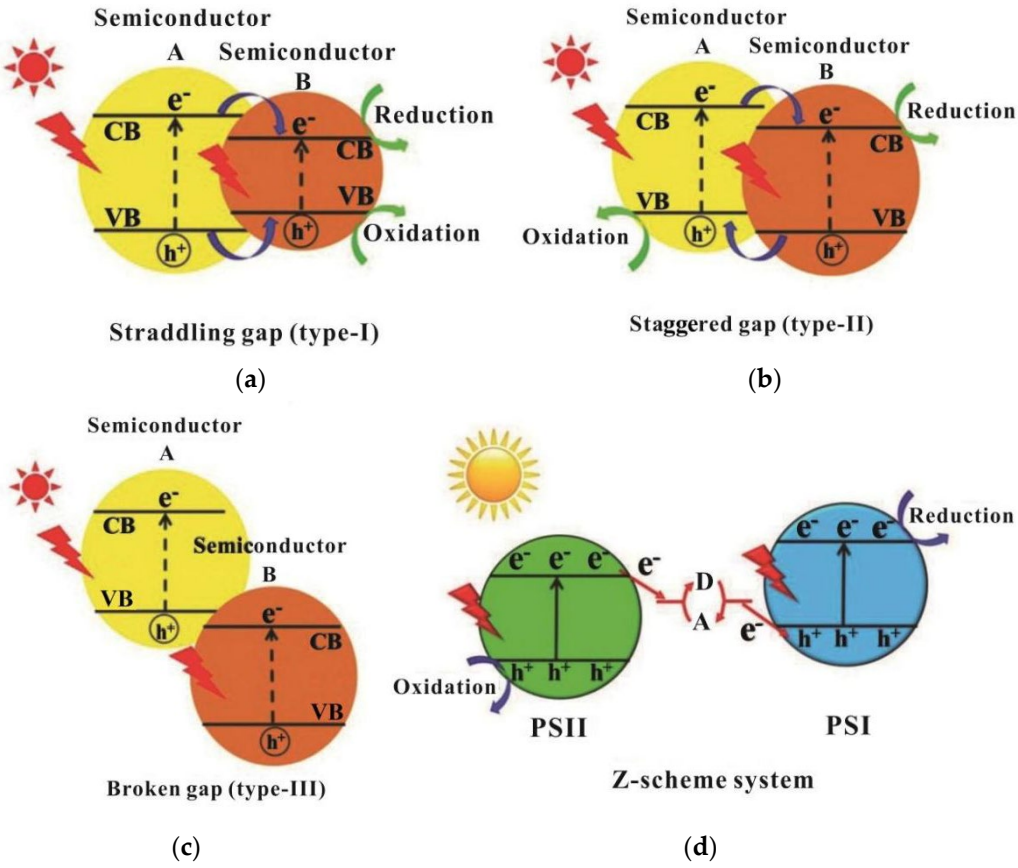

Figure 13. Schematic illustration on the separation ways of photogenerated electron-hole pairs over heterojunction photocatalysts: (**a**) type-I, (**b**) type-II, (**c**) type-III and (**d**) Z-scheme [142].

Graphene-TiO_2 composite has been widely studied because its excellent mobility of charge carriers, large specific surface area, flexible structure, high transparency, and good electrical and thermal conduction [148–154]. Zhang *et al.* [152] prepared TiO_2/graphene sheets composite by a sol-gel method, exhibiting a hydrogen evolution rate of 8.6 μmol h^{-1}, which was nearly two times that over the commercially available Degussa P25 (4.5 μmol.h^{-1}). Fu *et al.* [154] constructed a g-C_3N_4/graphene-CNTs/TiO_2 Z-scheme photocatalytic system, in which the graphene-CNTs effectively

Preprints (www.preprints.org) | NOT PEER-REVIEWED | Posted: 19 May 2023 doi:10.20944/preprints202305.1388.v1

promote the transfer of photogenerated carriers, thereby generating stronger photocurrent (Figure 14e,f).

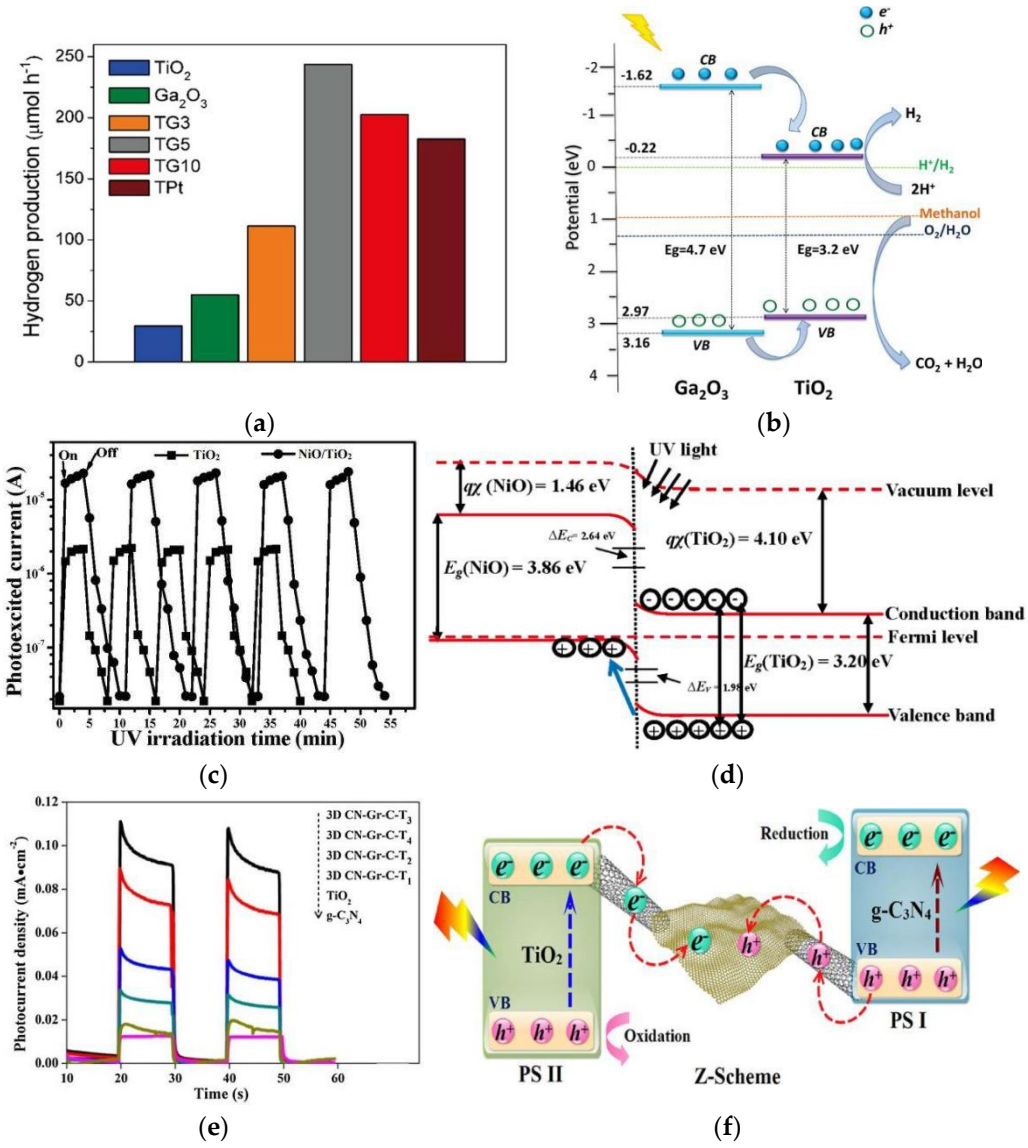

Figure 14. (**a**) Average hydrogen evolution rates of TiO_2, Ga_2O_3, TG3 (3% Ga_2O_3/TiO_2), TG5 (5% Ga_2O_3/TiO_2), TG10 (10% Ga_2O_3/TiO_2) photocatalysts and TPt reference (Pt modified TiO_2) [145]. (**b**) Mechanism for H_2 production over the TG5 photocatalyst [145]. (**c**) Transient current response curves of TiO_2 and NiO/TiO_2 nanocomposite under ultraviolet light irradiation [147]. (**d**) Schematic diagram on the energy band of a p-NiO/n-TiO_2 heterojunction structure [147]. (**e**) Transient current response curves of 3D g-C_3N_4/graphene-CNTs/TiO_2 samples with different amounts of TiO_2 under Xe lamp [154]. (**f**) Schematic diagram of the photocatalytic processes over 3D g-C_3N_4/graphene-CNTs/TiO_2 [154].

4.3. Surface Noble Metal Deposition

The photogenerated carriers will be redistributed when the surface semiconductor in contact with metal. The electrons will transfer from n-type semiconductor to metals because the lower Fermi levels of metals. Moreover, the surface plasmon polaritons can enhance the light response of TiO_2 [155–158]. In literature, Zheng *et al.* [159] investigated the photocatalytic performance of TiO_2 deposited with Au, Ag and AuAg bimetallic nanoparticles. The results showed that the local surface plasmon resonance of noble metals improved the photocatalytic activity TiO_2 under visible light irradiation. Luo *et al.* [160] reported a visible-light-driven responsive Au/rGO/hydrogenated TiO_2

Preprints (www.preprints.org) | NOT PEER-REVIEWED | Posted: 19 May 2023 doi:10.20944/preprints202305.1388.v1

nanotube arrays ternary composite with a high hydrogen evolution rate of 45 mmol cm^{-2} h^{-1}. The visible light harvesting was significantly improved by the Au nanoparticles due to the localized surface plasmon resonance effect. Ag and Pd have been also used to modify TiO_2 by depositing them on its surface [161–164]. For example, Ge *et al.* [161] decorated Ag nanoparticles onto vertically aligned TiO_2 nanotube arrays. The Ag decorated TiO_2 can efficiently drive photocatalytic water splitting under visible light irradiation owing to surface plasmon resonance of Ag (Figure 15).

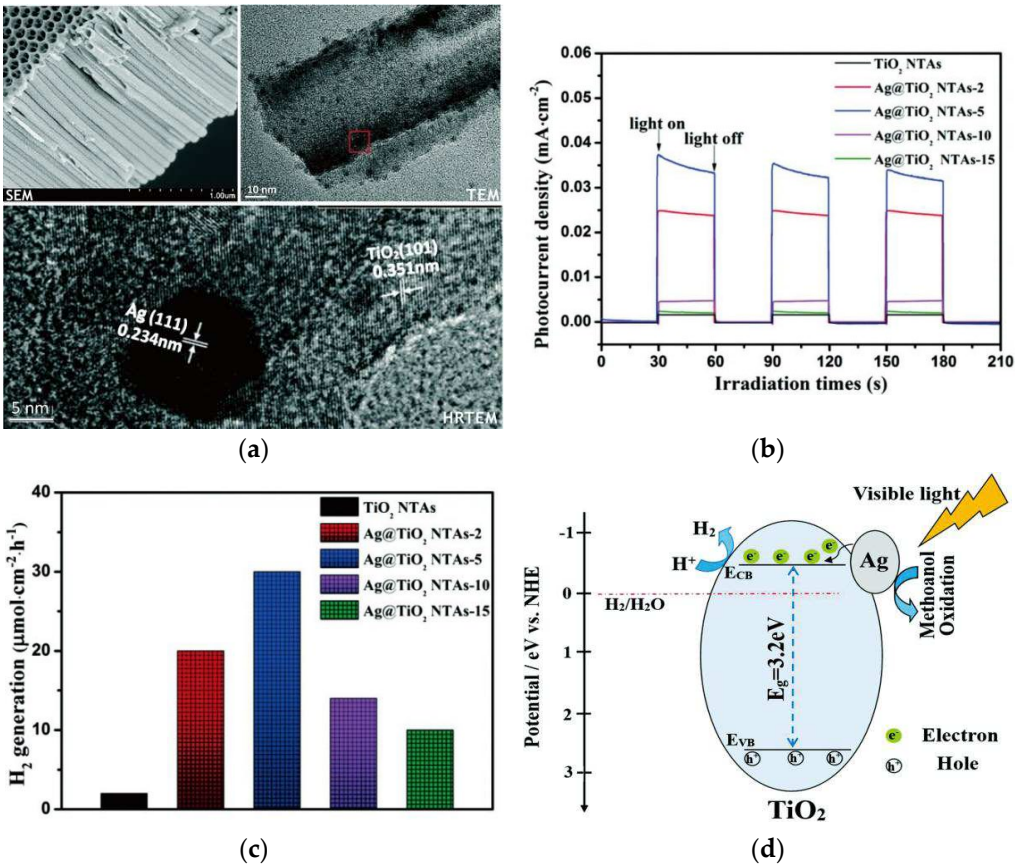

Figure 15. (**a**) SEM, TEM and HRTEM images of Ag@TiO_2 nanotube arrays (NTAs). (**b**) Photocurrent response curves of pure TiO_2 NTAs and Ag@TiO_2 NTAs prepared with different deposition times (2, 5, 10 and 15 min) under visible light irradiation. (**c**) Photocatalytic hydrogen evolution rate over pure TiO_2 NTAs and Ag@TiO_2 NTAs under the same conditions. (**d**) Schematic diagram on the energy band structure and the separation ways of photogenerated electron-hole pairs in Ag@TiO_2 NTAs under visible light irradiation [161].

4.4. Dye Sensitization

The excitation potential of some dyes is more negative than the CB potential of TiO_2. Thus the light response range of TiO_2 can be effectively expanded by dye sensitization. Dye molecules can deliver photogenerated electrons to the CB of TiO_2 and then the electrons transfer further to participate in reactions [165–167]. For example, Shi *et al.* [165] prepared Eosin Y-sensitized nanosheet-stacked hollow-sphere TiO_2 for efficient photocatalytic H_2 production under visible-light irradiation. Vallejo *et al.* [167] reported the enhancement on light absorption and photocatalytic activity over rGO-TiO_2 thin films after sensitized by natural dyes extracted from Bactris guineensis (Figure 16). In fact, lots of dyes have been used to sensitize TiO_2, such as complexes of Fe (II) and polypyridyl, quinacridone, hydroxoaluminum- tricarboxymonoamide phthalocyanine, and so on [168–170].

Preprints (www.preprints.org) | NOT PEER-REVIEWED | Posted: 19 May 2023 doi:10.20944/preprints202305.1388.v1

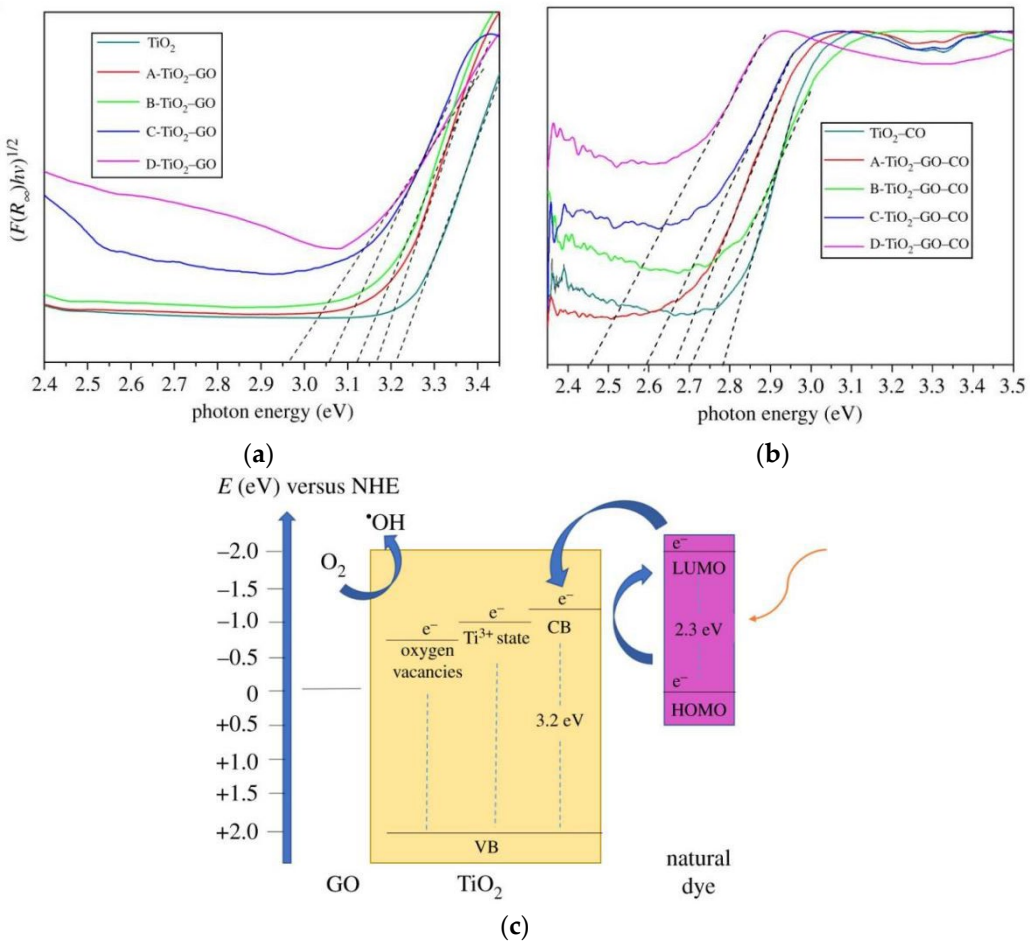

Figure 16. Band gaps estimated on the basis of the Kubelka-Munk plots for (**a**) TiO_2-GO thin films and (**b**) TiO_2-GO thin films sensitized with anthocyanin that was extracted from the fruit of Bactris guineensis (TiO_2-GO-CO). The samples A, B, C and D were prepared by extra adding 0.15%, 0.26%, 0.51% and 1.1% GO in mass into TiO_2. (**c**) Schematic illustration on the energy levels for the TiO_2-GO thin films sensitized with natural dye [167].

4.5. Loading on Supports

Loading on supports is an effective way to solve the problems of agglomeration and tough recycling of TiO_2 nanoparticles. In addition, the supporting materials of high electrical conductivity could provide channels for quick transfer of electrons, thereby decreasing the recombination rate of photogenerated e_{CB}^- and h_{VB}^+. For example, Li *et al.* [171] reported a catalyst of nitrogen-doped carbon nanofiber supporting MoS_2/TiO_2, in which the photogenerated electrons could quickly transfer to the carbon fiber along the basal plane of MoS_2 . In literature, zeolite, SiO_2, and carbon materials are frequently used as the supporting materials for TiO_2 [172–177]. Najafabadi *et al.* [175] reported four kinds of zeolites (Na-Y, Na-mordenite, H-Y, and H-beta) supporting TiO_2, which all exhibited high hydrogen evolution rate. Especially for the Na-Y zeolite supporting TiO_2, the rate reached 250.8 μmol g^{-1} h^{-1}, which is almost 3 times that of Degussa P25 (84.2 μmol g^{-1} h^{-1}) under the same conditions. Kim *et al.* [177] prepared TiO_2 supported by SiO_2, showing much higher photocatalytic activity than pure TiO_2, which can be attributed to the large specific surface area, Ti-O-Si bonds modified narrow band gap and the local structure. Loading on supports is frequently associated with other reactions like ion doping and forming heterojunctions. Thus it can combine the advantages of varied strategies. Yin *et al.* [178] synthesized Bi plasmon-enhanced mesoporous Bi_2MoO_6/Ti^{3+} self-doped TiO_2 microsphere heterojunctions. The formation of heterojunction, Ti^{3+} and surface plasmon resonance (SPR) of Bi jointly achieved high catalytical activity of TiO_2 under visible light. Xing *et al.* [179] combined ion doping with support and synthesized a F-doped-TiO_{2-x}/MCF composite, which exhibited high photocatalytic activity for hydrogen evolution.

Preprints (www.preprints.org) | NOT PEER-REVIEWED | Posted: 19 May 2023 doi:10.20944/preprints202305.1388.v1

4.6. Crystal Facet Engineering

The mainly exposed facets of traditional TiO_2 photocatalysts are the thermodynamically stable (101) facets. However, the specific surface energy of (001) facets is higher than that of (101) facets, implying that the (001) facets have higher reaction activity. In addition, the uncoordinated Ti_{5c} atoms in the (001) facets can narrow the band gap of TiO_2. Therefore, exposing more (001) facets will help to improve the photocatalytic performance of TiO_2, which is generally realized by controlling the synthesis conditions [180,181]. For instance, Wang *et al.* [182] synthesized a series of (001) facets dominated TiO_2 nanosheets with high visible-light photoactivity by a simple hydrothermal method at different temperatures. Shang *et al.* [183] synthesized graphene-TiO_2 nanocomposites with dominantly exposed (001) facets by various dosage of graphite oxide (GO) and hydrofluoric acid (HF) during a facile solvothermal process. The well conductive and highly reactive (001) facets enhanced the photocatalytic properties and facilitated the separation of photogenerated carriers.

As a summary, Table 2 lists the hydrogen evolution efficiency from photocatalytic water splitting over typical titanium oxide based photocatalysts. Obviously, noble metal modified TiO_2 photocatalysts have incomparable advantages on hydrogen evolution over the other titanium oxide based counterparts. But the searches for alternative non-noble metals are still one of the focuses in this field because of the high cost and scarcity of noble metals. Additionally, combining multiple modification methods can achieve better results than using a single method.

Table 2. Hydrogen evolution efficiency from photocatalytic water splitting over typical TiO_2-based photocatalysts.

Catalyst	Light Source	Reaction Condition	H_2 Production (mmol h^{-1})	Ref.
N-doped TiO_2	>400 nm	Water	0.315	[133]
N-doped TiO_2	>420 nm	EDTA-2Na solution	2.21	[132]
(B,N)-co-doped TiO_2	>420 nm	EDTA-2Na solution	10.45	[132]
(Sb,N)-co-doped TiO_2	Xe lamp	10% aqueous TEOA solution	2.33	[184]
B-doped TiO_2	365 nm	0.2 M HCl and absolute ethanol aqueous solution (1:1)	0.099	[135]
N-doped TiO_2	visible light	H_2S/0.25 M KOH solution	8.8	[130]
N-doped TiO_2	Xe lamp	20% aqueous methanol solution	2.98	[129]
S-doped TiO_2	Xe lamp	1 M NaOH aqueous solution	0.17	[134]
Fe-doped TiO_2	solar light radiation	triammonium phosphate aqueous solution	4.01	[139]
Co-doped TiO_2	solar light radiation	triammonium phosphate aqueous solution	9.82	[139]
(Fe,Co)-co-doped TiO_2	solar light radiation	triammonium phosphate aqueous solution	17.41	[139]
La-doped TiO_2	Hg UVA lamp	12 M aqueous methanol solution	80	[185]
Ce-doped TiO_2	visible light	sulphide wastewater from refinery	6.789	[186]
H-doped TiO_2	365 nm	25% aqueous methanol solution	0.286	[140]
F-doped TiO_2	365 nm	25% aqueous methanol solution	0.0928	[140]
Cl-doped TiO_2	365 nm	25% aqueous methanol solution	0.336	[140]
V-doped TiO_2/rGO	Xe lamp	20% aqueous methanol solution	0.12	[187]
N-doped Ni/C/TiO_2	Hg lamp	30% aqueous methanol solution	0.383	[188]
Sr-doped $TiO_{2-\delta}$	>400 nm	water	1.092	[189]
$TiO_{2-\delta}$	>420 nm	30% aqueous methanol solution	0.00058	[190]
Pt/$TiO_{2-\delta}$	visible light	50% aqueous methanol solution	4.9	[63]
Ag-decorated TiO_2	Hg lamp	water	120	[191]
Au-decorated TiO_2	254 nm	aqueous methanol solution	106	[163]
Au,Pd-decorated TiO_2	254 nm	aqueous methanol solution	266	[163]
Au,Ni-decorated TiO_2	254 nm	aqueous methanol solution	256	[163]
Au,Co-decorated TiO_2	254 nm	aqueous methanol solution	171	[163]
Pd-decorated TiO_2	254 nm	aqueous methanol solution	59	[163]
Ni-decorated TiO_2	254 nm	aqueous methanol solution	20	[163]

Preprints (www.preprints.org) | NOT PEER-REVIEWED | Posted: 19 May 2023 doi:10.20944/preprints202305.1388.v1

Co-decorated TiO_2	254 nm	aqueous methanol solution	10	[163]
$Cu(OH)_2/TiO_2$	ultraviolet light	10% aqueous methanol solution	14.94	[192]
Cu/TiO_2	UV lamp	25% aqueous methanol solution	5	[193]
Cu/TiO_2	visible light	25% aqueous methanol solution	0.22	[193]
Co_3O_4@C/TiO_2	365 nm	25% aqueous methanol solution	11.4	[194]
NiO/TiO_2	Hg lamp	glycerol and distilled water	1.2	[195]
g-C_3N_4/N-TiO_2	Xe lamp	20% aqueous methanol solution	8.931	[34]
EosinY-sensitized TiO_2/ZrO_2	Xe arc lamp	15% DEA aqueous solution	1.87	[196]
β-Ga_2O_3/TiO_2	254 nm	50% aqueous methanol solution	0.244	[145]
N-doped TiO_2/N-doped graphene	Xe lamp	10% aqueous TEOA solution	0.039	[197]
FeO-TiO_2/ACF	visible light	20% aqueous methanol solution	6.178	[198]
TiO_2/ACF	visible light	20% aqueous methanol solution	1.672	[198]
Cu-doped TiO_2 with preferred (001) orientation	Xe lamp	10% aqueous methanol solution	0.81	[199]
g-C_3N_4/TiO_2 with preferred (001) orientation	>420 nm	10% aqueous TEOA solution	0.033	[200]
TiO_2/graphene with exposed (001) facets	Xe lamp	25% aqueous methanol solution	0.736	[201]

5. Conclusions and Outlooks

(1) Oxygen-deficient titanium oxide ($TiO_{2-\delta}$) shows higher photocatalytic activity than stoichiometric TiO_2, which can be mainly attributed to the presence of Ti^{3+} species and oxygen deficiencies. The Ti^{3+} species would lead to new intermediate defect states (shallow donor), forming below the bottom of conduction band of TiO_2, which thus narrows the band gap of TiO_2. The presence of oxygen deficiencies can decrease the transfer resistance of electrons. Resultantly, the photogenerated electrons can quickly transfer, thereby avoiding recombining with holes.

(2) Reductive treatment is the most direct and effective method to introduce oxygen defects in titanium oxides, for which H_2 is the commonest reductant, while other reductants like carbon, $NaBH_4$ and NH_3 can also be selected. Moreover, ion doping, pulsed laser irradiation, calcination under anoxic conditions, plasma assistance and so forth have also been proven efficient strategies for introducing oxygen defects into titanium oxides. Other modification methods for TiO_2, including ion doping, composite, surface noble metal deposition, dye sensitization and loading on supports, are also exploited to broaden the light absorption region and suppress the recombination of photogenerated e_{CB^-} and h_{VB^+} for $TiO_{2-\delta}$. The photocatalytic activity of titanium oxides is hopefully improved further by the combination of introducing oxygen defects with these modification methods, which have reached some remarkable results.

(3) Hydrogen production by photocatalytic water splitting over $TiO_{2-\delta}$ based photocatalyst shows a strong development momentum. But there exist at least two major challenges at present. The first is how to control the concentration of oxygen defects in $TiO_{2-\delta}$. Although the density of oxygen deficiencies can be controlled by adjusting the conditions of reduction treatment, the spontaneously introduced oxygen defects during other modification processes like ion doping and surface treatment is difficult to control and predict accurately. Thus, choosing an appropriate synthesis method is very important to prepare $TiO_{2-\delta}$ based photocatalysts. Secondly, the present researches on regulating energy band structure mainly concentrate on enhancing light harvesting. Actually, the positions of CB and VB are also very critical for photocatalytic water splitting, especially the position of CB. The CB position of TiO_2 is very close to the reduction potential of H^+/H_2 (0 V vs. NHE at pH=0). The decrease of CB minimum can lead to a wider light absorption region, but the reducing ability of photogenerated electrons is also impaired at the same time. If the CB minimum is more positive than the reduction potential of H^+/H_2, the photocatalytic hydrogen evolution activity will take a mighty blow. Thus, regulating the band gap of TiO_2 is really a challenging task, because there are numerous factors that can affect the band position of $TiO_{2-\delta}$ during the modifying process. Combining theoretical calculation prediction with precise control of synthesis conditions may be a solution to solve this

issue. In addition, the present researches pay little attention to the adsorption of reactant (H_2O) and the desorption of products (H_2 and O_2). In fact, these two processes are also very crucial for the whole photocatalytic hydrogen evolution, which might be the next hot topic in researches. Although photocatalytic hydrogen evolution is still remained in laboratory stage, it is hopefully fruitful and prosperous with deep researches.

Author Contributions: Y.C.: literature surveying, drawing of figures and tables, sorting data, writing of original manuscript; X.F.: literature surveying, revision and finalizing of the manuscript; Z.P.: revision and finalizing of the manuscript. All authors have read and agreed to the published version of the manuscript.

Funding: Many thanks for the financial support to this work by National Natural Science Foundation of China (grant nos. 12174035 and 61274015).

Conflicts of Interest: The authors declare no conflict of interest.

Reference

1. Akorede, M.F.; Hizam, H.; Pouresmaeil, E. Distributed energy resources and benefits to the environment. *Renewable & Sustainable Energy Reviews*, **2010**, 14 (2), 724-734.
2. Aslan, M.; Isik, H. Green energy for the battlefield. *International Journal of Green Energy*, **2017**, 14 (12), 1020-1026.
3. Dorian, J.P.; Franssen, H.T.; Simbeck, D.R. Global challenges in energy. *Energy Policy*, **2006**, 34 (15), 1984-1991.
4. Koroneos, C.; Spachos, T.; Moussiopoulos, N. Exergy analysis of renewable energy sources. *Renewable Energy*, **2003**, 28 (2), 295-310.
5. Kumar, G.; Kim, S.H.; Lay, C.H.; Ponnusamy, V.K. Recent developments on alternative fuels, energy and environment for sustainability Preface. *Bioresource Technology*, **2020**, 317, 124010.
6. Mulligan, S. Energy, Environment, and Security: Critical Links in a Post-Peak World. *Global Environmental Politics*, **2010**, *10* (4), 79-100.
7. Veziroglu, T.N.; Sahin, S. 21st Century's energy: Hydrogen energy system. *Energy Conversion and Management*, **2008**, 49 (7), 1820-1831.
8. Momirlan, M.; Veziroglu, T.N. The properties of hydrogen as fuel tomorrow in sustainable energy system for a cleaner planet. *International Journal of Hydrogen Energy*, **2005**, 30 (7), 795-802.
9. Sartbaeva, A.; Kuznetsov, V.L.; Wells, S.A.; Edwards, P.P. Hydrogen nexus in a sustainable energy future. *Energy & Environmental Science*, **2008**, 1 (1), 79-85.
10. Midilli, A.; Dincer, I. Hydrogen as a renewable and sustainable solution in reducing global fossil fuel consumption. *International Journal of Hydrogen Energy*, **2008**, 33 (16), 4209-4222.
11. Muradov, N. Low to near-zero CO2 production of hydrogen from fossil fuels: Status and perspectives. *International Journal of Hydrogen Energy*, **2017**, 42 (20), 14058-14088.
12. Rosen, M.A. Combating global warming via non-fossil fuel energy options. *International Journal of Global Warming*, **2009**, 1 (1-3), 2-28.
13. Wang, Z.; Naterer, G.F. Integrated fossil fuel and solar thermal systems for hydrogen production and CO2 mitigation. *International Journal of Hydrogen Energy*, **2014**, 39 (26), 14227-14233.
14. Sapountzi, F.M.; Gracia, J.M.; Weststrate, C.J.; Fredriksson, H.O.A.; Niemantsverdriet, J.W. Electrocatalysts for the generation of hydrogen, oxygen and synthesis gas. *Progress in Energy and Combustion Science*, **2017**, 58, 1-35.
15. Tee, S.Y.; Win, K.Y.; Teo, W.S.; Koh, L.D.; Liu, S.; Teng, C.P.; Han, M.Y. Recent Progress in Energy-Driven Water Splitting. *Advanced Science*, **2017**, 4 (5), 1600337.
16. Fujishima, A.; Honda, K. Electrochemical photolysis of water at a semiconductor electrode. *Nature*, **1972**, *238* (5358), 37-38.
17. Faraji, M.; Yousefi, M.; Yousefzadeh, S.; Zirak, M.; Naseri, N.; Jeon, T.H.; Choi, W.; Moshfegh, A.Z. Two-dimensional materials in semiconductor photoelectrocatalytic systems for water splitting. *Energy & Environmental Science*, **2019**, 12 (1), 59-95.
18. Gholipour, M.R.; Cao-Thang, D.; Beland, F.; Trong-On, D. Nanocomposite heterojunctions as sunlight-driven photocatalysts for hydrogen production from water splitting. *Nanoscale*, **2015**, 7 (18), 8187-8208.
19. Ismail, A.A.; Bahnemann, D.W. Photochemical splitting of water for hydrogen production by photocatalysis: A review. *Solar Energy Materials and Solar Cells*, **2014**, 128, 85-101.
20. Bich Ha, N.; Van Hieu, N.; Dinh Lam, V. Photocatalytic composites based on titania nanoparticles and carbon nanomaterials. *Advances in Natural Sciences-Nanoscience and Nanotechnology*, **2015**, 6 (3), 033001.
21. Chan, S.H.S.; Wu, T.Y.; Juan, J.C.; Teh, C.Y. Recent developments of metal oxide semiconductors as photocatalysts in advanced oxidation processes (AOPs) for treatment of dye waste-water. *Journal of Chemical Technology and Biotechnology*, **2011**, 86 (9), 1130-1158.

22. Djurisic, A.B.; He, Y.; Ng, A.M.C. Visible-light photocatalysts: Prospects and challenges. *APL Materials*, **2020**, *8* (3) 030903.
23. Yang, Y.; Yin, L.C.; Gong, Y.; Niu, P.; Wang, J.Q.; Gu, L.; Chen, X.; Liu, G.; Wang, L.; Cheng, H.M. An Unusual Strong Visible-Light Absorption Band in Red Anatase TiO_2 Photocatalyst Induced by Atomic Hydrogen-Occupied Oxygen Vacancies. *Advanced Materials*, **2018**, 30 (6) 1704479.
24. Cushing, S.K.; Meng, F.K.; Zhang, J.Y.; Ding, B.F.; Chen, C.K.; Chen, C.J.; Liu, R.S.; Bristow, A.D.; Bright, J.; Zheng, P.; Wu, N.Q. Effects of defects on photocatalytic activity of hydrogen-treated titanium oxide nanobelts. *ACS Catal*, **2017**, 7(3), 1742-1748.
25. Tian, M.; Mahjouri-Samani, M.; Eres, G.; Sachan, R.; Yoon, M.; Chisholm, M.F.; Wang, K.; Puretzky, A.A.; Rouleau, C.M.; Geohegan, D.B.; Duscher, G. Structure and Formation Mechanism of Black TiO_2 Nanoparticles. *ACS Nano*, **2015**, 9 (10), 10482-10488.
26. Hong, R.J.; Deng, C.; Jing, M.; Lin, H.; Tao, C.X.; Zhang, D.W. Oxygen flows-dependent photocatalytic performance in Ti^{3+} doped TiO_2 thin films. *Optical Materials*, **2019**, 95:109224 .
27. Nakajima, T.; Nakamura, T.; Shinoda, K.; Tsuchiya, T. Rapid formation of black titania photoanodes: pulsed laser-induced oxygen release and enhanced solar water splitting efficiency. *Journal of Materials Chemistry A*, **2014**, 2 (19), 6762-6771.
28. Yuan, K.; Cao, Q.; Lu, H.L.; Zhong, M.; Zheng, X.; Chen, H.Y.; Wang, T.; Delaunay, J.J.; Luo, W.; Zhang, L.; Wang, Y.Y.; Deng, Y.; Ding, S.J.; Zhang, D.W. Oxygen-deficient WO_{3-x}@TiO_{2-x} core-shell nanosheets for efficient photoelectrochemical oxidation of neutral water solutions. *Journal of Materials Chemistry A*, **2017**, 5 (28), 14697-14706.
29. Zhao, Z.; H. Tan, Q.; Zhao, H. F.; Lv, Y.; Zhou, L. J.; Song, Y. J.; Sun, Z. C. Reduced TiO_2 rutile nanorods with well-defined facets and their visible-light photocatalytic activity. *Chemical Communications*, **2014**, *50*(21), 2755-2757.
30. Wang Y.Q.; Yu X.J.; Sun D.Z.. Synthesis, characterization, and photocatalytic activity of $TiO_{2-x}N_x$ nanocatalyst. *Journal of Hazardous Materials*, **2007**, 144 (1-2): 328-333.
31. Yuan, J.; Liu, Y.Y.; Bo, T.T.; Zhou, W. Activated HER performance of defected single layered TiO_2 nanosheet via transition metal doping. *International Journal of Hydrogen Energy*, **2020**, 45(4), 2681-2688.
32. Liu, G.; Yang, H.G.; Wang, X.; Cheng, L.; Lu, H.; Wang, L.; Lu, G.Q.; Cheng, H.M. Enhanced photoactivity of oxygen-deficient anatase TiO_2 sheets with dominant {001} facets. *Journal of Physical Chemistry C*, **2009**, 113 (52), 21784-21788.
33. Weng, X.L.; Zhang, Y.L.; Dong, F.; Wu, Z.B.; Darr, J.A. Thermocatalytic syntheses of highly defective hybrid nano-catalysts for photocatalytic hydrogen evolution. *Journal of Materials Chemistry A*, **2017**, 5(45), 23766-23775.
34. Han, C.; Wang, Y.D.; Lei, Y.P.; Wang, B.; Wu, N.; Shi, Q.; Li, Q. In situ synthesis of graphitic-C_3N_4 nanosheet hybridized N-doped TiO_2 nanofibers for efficient photocatalytic H_2 production and degradation. *Nano Research*, **2015**, 8(4), 1199-1209.
35. Rajeshwar, K. Hydrogen generation at irradiated oxide semiconductor-solution interfaces. *Journal of Applied Electrochemistry*, **2007**, 37(7), 765-787.
36. Palmisano, G.; Augugliaro, V.; Pagliaro, M.; Palmisano, L. Photocatalysis: a promising route for 21st century organic chemistry. *Chemical Communications*, **2007**, (33), 3425-3437.
37. Lettieri, S.; Pavone, M.; Fioravanti, A.; Santamaria Amato, L.; Maddalena, P. Charge carrier processes and optical properties in TiO_2 and TiO_2-based heterojunction photocatalysts: A review. *Materials*, **2021**, 14 (7), 1645.
38. Nakano, T.; Ito, R.; Kogoshi, S.; Katayama, N. Optimal levels of oxygen deficiency in the visible light photocatalyst TiO_{2-x} and long-term stability of catalytic performance. *Journal of Physics and Chemistry of Solids*, **2016**, 98, 136-142.
39. Wu, H.; Wang, Z.; Jin, S.; Cao, X.; Ren, F.; Wu, L.; Xing, Z.; Wang, X.; Cai, G.; Jiang, C. Jiang. Enhanced photoelectrochemical performance of TiO_2 through controlled Ar^+ ion irradiation: A combined experimental and theoretical study. *International Journal of Hydrogen Energy*, **2018**, 43 (14), 6936-6944.
40. Amano, F.; Nakata, M.; Yamamoto, A.; Tanaka, T. Effect of Ti^{3+} ions and conduction band electrons on photocatalytic and photoelectrochemical activity of rutile titania for water oxidation. *Journal of Physical Chemistry C*, **2016**, 120 (12), 6467-6474.
41. Singh, A.P.; Kodan, N.; Mehta, B.R. Enhancing the photoelectrochemical properties of titanium dioxide by thermal treatment in oxygen deficient environment. *Applied Surface Science*, **2016**, 372, 63-69.
42. Li, Y.; Cooper, J.K.; Liu, W.; Sutter-Fella, C.M.; Amani, M.; Beeman, J.W.; Javey, A.; Ager, J.W.; Liu, Y.; Toma, F.M.; Sharp, I.D. Defective TiO_2 with high photoconductive gain for efficient and stable planar heterojunction perovskite solar cells. *Nature Communications*, **2016**, 7, 12446.
43. Hao, Z.; Chen, Q.; Dai, W.; Ren, Y.; Zhou, Y.; Yang, J.; Xie, S.; Shen, Y.; Wu, J.; Chen, W.; Xu, G.Q. Oxygen-deficient blue TiO_2 for ultrastable and fast lithium storage. *Advanced Energy Materials*, **2020**, 10 (10), 1903107.

44. Wendt, S.; Sprunger, P.T.; Lira, E.; Madsen, G.K.H.; Li, Z.; Hansen, J.O.; Matthiesen, J.; Blekinge-Rasmussen, A.; Laegsgaard, E.; Hammer, B.; Besenbacher, F. The role of interstitial sites in the Ti3d defect state in the band gap of Titania. *Science*, **2008**, 320 (5884), 1755-1759.
45. Long, Z.; Li, Q.; Wei, T.; Zhang, G.; Ren, Z. Historical development and prospects of photocatalysts for pollutant removal in water. *Journal of Hazardous Materials*, **2020**, 395, 122599.
46. Tang, L.; Sallet, D.; Lemaire, J. Photochemistry of polyundecanamides 2. TiO_2-photocatalyzed and zno-photocatalyzed oxidation. *Macromolecules*, **1982**, 15 (5), 1437-1441.
47. Baba, R.; Nakabayashi, S.; Fujishima, A.; Honda, K. Investigation of the mechanism of hydrogen evolution during photocatalytic water decomposition on metal-loaded semiconductor powders. *Journal of Physical Chemistry*, **1985**, 89 (10), 1902-1905.
48. Matthews, R.W. Photooxidation of organic impurities in water using thin-films of titanium-dioxide. *Journal of Physical Chemistry*, **1987**, 91 (12), 3328-3333.
49. Wagner, N.; Brummer, O.; Sauer, N. Photoemission-studies of titanium-oxides. *Crystal Research and Technology*, **1982**, 17 (9), 1151-1158.
50. Sasikala, R.; Sudarsan, V.; Sudakar, C.; Naik, R.; Sakuntala, T.; Bharadwaj, S.R. Enhanced photocatalytic hydrogen evolution over nanometer sized Sn and Eu doped titanium oxide. *International Journal of Hydrogen Energy*, **2008**, 33 (19), 4966-4973.
51. Amano, F.; Nakata, M. High-temperature calcination and hydrogen reduction of rutile TiO_2: A method to improve the photocatalytic activity for water oxidation. *Applied Catalysis B-Environmental*, **2014**, 158, 202-208.
52. Mali, M.G.; Yoon, H.; An, S.; Choi, J.Y.; Kim, H.Y.; Lee, B.C.; Kim, B.N.; Park, J.H.; Al-Deyab, S.S.; Yoon, S.S. Enhanced solar water splitting of electron beam irradiated titania photoanode by electrostatic spray deposition. *Applied Surface Science*, **2014**, 319, 205-210.
53. Pitchaimuthu, S.; Honda, K.; Suzuki, S.; Naito, A.; Suzuki, N.; Katsumata, K.i.; Nakata, K.; Ishida, N.; Kitamura, N.; Idemoto, Y.; Kondo, T.; Yuasa, M.; Takai, O.; Ueno, T.; Saito, N.; Fujishima, A.; Terashima, C. Solution plasma process-derived defect-induced heterophase anatase/brookite TiO_2 nanocrystals for enhanced gaseous photocatalytic performance. *ACS Omega*, **2018**, 3 (1), 898-905.
54. Ennaceri, H.; Boujnah, M.; Taleb, A.; Khaldoun, A.; Saez-Araoz, R.; Ennaoui, A.; El Kenz, A.; Benyoussef, A. Thickness effect on the optical properties of TiO_2-anatase thin films prepared by ultrasonic spray pyrolysis: Experimental and ab initio study. *International Journal of Hydrogen Energy*, **2017**, 42 (30), 19467-19480.
55. Amano, F.; Yasumoto, T.; Prieto-Mahaney, O.O.; Uchida, S.; Shibayama, T.; Ohtani, B. Photocatalytic activity of octahedral single-crystalline mesoparticles of anatase titanium(IV) oxide. *Chemical Communications*. **2009**, (17),2311-2313..
56. Chen, Y.; Cao, X.; Lin, B.; Gao, B. Origin of the visible-light photoactivity of NH_3-treated TiO_2: Effect of nitrogen doping and oxygen vacancies. *Applied Surface Science*, **2013**, 264, 845-852.
57. Leichtweiss, T.; Henning, R.A.; Koettgen, J.; Schmidt, R.M.; Hollaender, B.; Martin, M.; Wuttig, M.; Janek, J. Amorphous and highly nonstoichiometric titania (TiO_x) thin films close to metal-like conductivity. *Journal of Materials Chemistry A*, **2014**, 2 (18), 6631-6640.
58. Zhang, Y.X.; Wu, S.M.; Tian, G.; Zhao, X.F.; Wang, L.Y.; Yin, Y.X.; Wu, L.; Li, Q.N.; Zhang, Y.X.; Wu, J.S.; Janiak, C.; Ozoemena, K.I.; Shalom, M.; Yang, X.Y. Titanium vacancies in TiO_2 nanofibers enable highly efficient photodriven seawater splitting. *Chemistry-A European Journal*, **2021**, 27(57), 14202-14208.
59. An, X.; Hu, C.; Liu, H.; Qu, J. Oxygen vacancy mediated construction of anatase/brookite heterophase junctions for high-efficiency photocatalytic hydrogen evolution. *Journal of Materials Chemistry A*, **2017**, 5 (47), 24989-24994.
60. Zhang, K.; Zhou, W.; Chi, L.; Zhang, X.; Hu, W.; Jiang, B.; Pan, K.; Tian, G.; Jiang, Z. Black N/H-TiO_2 nanoplates with a flower-like hierarchical architecture for photocatalytic hydrogen evolution. *Chemsuschem*, **2016**, 9 (19), 2841-2848.
61. Qiu, J.Y.; Feng, H.Z.; Chen, Z.H.; Ruan, S.H.; Chen, Y.P.; Xu, T.T.; Su, J.Y.; Ha, E.N.; Wang, L.Y. Selective introduction of surface defects in anatase TiO_2 nanosheets for highly efficient photocatalytic hydrogen generation. *Rare Metals*, **2022**, 41(6), 2074-2083.
62. Yuan, D.; Jiao, Y.; Li, Z.; Chen, X.; Ding, J.; Dai, W.L.; Wan, H.; Guan, G. TiN bridged all-Solid Z-Scheme CNNS/TiN/TiO_{2-x} heterojunction by a facile in situ reduction strategy for enhanced photocatalytic hydrogen evolution. *Advanced Materials Interfaces*, **2021**, 8 (16),: 2100695.
63. Yamazaki, Y.; Mori, K.; Kuwahara, Y.; Kobayashi, H.; Yamashita, H. Defect engineering of Pt/TiO_{2-x} photocatalysts via reduction treatment assisted by hydrogen spillover. *ACS Applied Materials & Interfaces*, **2021**, 13(41), 48669-48678.
64. Jia, G.R.; Wang, Y.; Cui, X.Q.; Zhang, H.Z.; Zhao, J.X.; Li, L.H.; Gu, L.; Zhang, Q.H.; Zheng, L.R.; Wu, J.D.; Wu, Q.; Singh, D.J.; Li, W.W.; Zhang, L.; Zheng, W.T. Wet-chemistry hydrogen doped TiO_2 with switchable defects control for photocatalytic hydrogen evolution. *Matter*, **2022**, 5(1), 206-218.

65. Park, E.; Patil, S.S.; Lee, H.; Kumbhar, V.S.; Lee, K. Photoelectrochemical H_2 evolution on $WO_3/BiVO_4$ enabled by single-crystalline TiO_2 overlayer modulations. *Nanoscale*, **2021**, 13(40), 16932-16941.
66. Hu, X.; Song, J.; Luo, J.; Zhang, H.; Sun, Z.; Li, C.; Zheng, S.; Liu, Q. Single-atomic Pt sites anchored on defective TiO_2 nanosheets as a superior photocatalyst for hydrogen evolution. *Journal of Energy Chemistry*, **2021**, 62, 1-10.
67. Mo, L.B.; Bai, Y.; Xiang, Q.Y.; Li, Q.; Wang, J.O.; Ibrahim, K.; Cao, J.L. Band gap engineering of TiO_2 through hydrogenation. *Applied Physics Letters*, **2014**, 105(20), 202114.
68. Wang, H.; Wang, G.; Ling, Y.; Lepert, M.; Wang, C.; Zhang, J.Z.; Li, Y. Photoelectrochemical study of oxygen deficient TiO_2 nanowire arrays with CdS quantum dot sensitization. *Nanoscale*, **2012**, 4(5), 1463-1466.
69. Liu, N.; Zhou, X.M.; Nguyen, N.T.; Peters, K.; Zoller, F.; Hwang, I.; Schneider, C.; Miehlich, M.E.; Freitag, D.; Meyer, K.; Fattakhova-Rohlfing, D.; Schmuki, P. Black magic in gray titania: noble-metal-free photocatalytic H_2 evolution from hydrogenated anatase. *ChemSusChem*, **2017**, 10(1), 62-67.
70. Xu, Y.F.; Zhang, C.; Zhang, L.X.; Zhang, X.H.; Yao, H.L.; Shi, J.L. Pd-catalyzed instant hydrogenation of TiO_2 with enhanced photocatalytic performance. *Energy & Environmental Science*, **2016**, 9(7), 2410-2417.
71. Zhang, J.W.; Wang, S.; Liu, F.S.; Fu, X.J.; Ma, G.Q.; Hou, M.S.; Tang, Z. Preparation of defective TiO_{2-x} hollow microspheres for photocatalytic degradation of methylene blue. *Acta Physico-Chimica Sinica*, **2019**, 35(8), 8 885-895.
72. Wierzbicka, E.; Altomare, M.; Wu, M.J.; Liu, N.; Yokosawa, T.; Fehn, D.; Qin, S.S.; Meyer, K.; Unruh, T.; Spiecker, E.; Palmisano, L.; Bellardita, M.; Will, J.; Schmuki, P. Reduced grey brookite for noble metal free photocatalytic H_2 evolution. *Journal of Materials Chemistry A*, **2021**, 9(2), 1168-1179.
73. Samsudin, E.M.; Hamid, S.B.A.; Juan, J.C.; Basirun, W.J.; Kandjani, A.E. Surface modification of mixed-phase hydrogenated TiO_2 and corresponding photocatalytic response. *Applied Surface Science*, **2015**, 359, 883-896.
74. Ihara, T.; Miyoshi, M.; Iriyama, Y.; Matsumoto, O.; Sugihara, S. Visible-light-active titanium oxide photocatalyst realized by an oxygen-deficient structure and by nitrogen doping. *Applied Catalysis B-Environmental*, **2003**, 42 (4), 403-409.
75. Guan, S.; Hao, L.; Lu, Y.; Yoshida, H.; Pan, F.; Asanuma, H. Fabrication of oxygen-deficient TiO_2 coatings with nano-fiber morphology for visible-light photocatalysis. *Materials Science in Semiconductor Processing*, **2016**, 41, 358-363.
76. Zhao, H.; Chen, J.; Rao, G.; Deng, W.; Li, Y. Enhancing photocatalytic CO_2 reduction by coating an ultrathin Al_2O_3 layer on oxygen deficient TiO_2 nanorods through atomic layer deposition. *Applied Surface Science*, **2017**, 404, 49-56.
77. Martinez-Oviedo A.; Ray, S.K.; Hoang Phuc, N.; Lee, S.W. Efficient photo-oxidation of NO_x by Sn doped blue TiO_2 nanoparticles. *Journal of Photochemistry and Photobiology A-Chemistry*, **2019**, 370, 18-25.
78. Pereira, A.L.J.; Lisboa Filho, P.N.; Acuna, J.; Brandt, I.S.; Pasa, A.A.; Zanatta, A.R.; Vilcarromero, J.; Beltran, A.; Dias da Silva, J.H. Enhancement of optical absorption by modulation of the oxygen flow of TiO_2 films deposited by reactive sputtering. *Journal of Applied Physics*, **2012**, 111 (11), 113513.
79. Dhumal, S.Y.; Daulton, T.L.; Jiang, J.; Khomami, B.; Biswas, P. Synthesis of visible light-active nanostructured TiO_x ($x < 2$) photocatalysts in a flame aerosol reactor. *Applied Catalysis B-Environmental*, **2009**, 86 (3-4), 145-151.
80. Xiao, P.; Liu, D.W.; Garcia, B.B.; Sepehri, S.; Zhang, Y.H.; Cao, G.Z. Electrochemical and photoelectrical properties of titania nanotube arrays annealed in different gases. *Sensors and Actuators B-Chemical*, **2008**, 134 (2), 367-372.
81. Kushwaha, S.; Nagarajan, R. Black TiO_2-graphitic carbon nanocomposite from a single source precursor and its interaction with colored and colorless contaminants under visible radiation. *Materials Research Bulletin*, **2020**, 132, 110983.
82. Starbova, K.; Yordanova, V.; Nihtianova, D.; Hintz, W.; Tomas, J.; Starbov, N. Excimer laser processing as a tool for photocatalytic design of sol-gel TiO_2 thin films. *Applied Surface Science*, **2008**, 254 (13), 4044-4051.
83. Wang, Z.; Yang, C.Y.; Lin, T.Q.; Yin, H.; Chen, P.; Wan, D.Y.; Xu, F.F.; Huang, F.Q.; Lin, J H.; Xie, X.M.; Jiang, M.H. H-doped black titania with very high solar absorption and excellent photocatalysis enhanced by localized surface plasmon resonance. *Advanced Functional Materials*, **2013**, 23(43), 5444-5450.
84. Filice, S.; Fiorenza, R.; Reitano, R.; Scalese, S.; Scire, S.; Fisicaro, G.; Deretzis, I.; La Magna, A.; Bongiorno, C.; Compagnini, G. TiO_2 colloids laser-treated in ethanol for photocatalytic H_2 production. *ACS Applied Nano Materials*, **2020**, 3(9), 9127-9140.
85. Fiorenza, R.; Scire, S.; D'Urso, L.; Compagnini, G.; Bellardita, M.; Palmisano, L. Efficient H_2 production by photocatalytic water splitting under UV or solar light over variously modified TiO_2-based catalysts. *International Journal of Hydrogen Energy*, **2019**, 44(29), 14796-14807.
86. Nakajima, T.; Tsuchiya, T.; Kumagai, T. Pulsed laser-induced oxygen deficiency at TiO_2 surface: Anomalous structure and electrical transport properties. *Journal of Solid State Chemistry*, **2009**, 182(9), 2560-2565.

87. Kunti, A.K.; Chowdhury, M.; Sharma, S.K.; Gupta, M.; Chaudhary, R.J. Influence of O_2 pressure on structural, morphological and optical properties of TiO_2-SiO_2 composite thin films prepared by pulsed laser deposition. *Thin Solid Films*, **2017**, 629, 79-89.
88. Ali, N.; Bashir, S.; Umm i, K.; Akram, M.; Mahmood, K. Effect of dry and wet ambient environment on the pulsed laser ablation of titanium. *Applied Surface Science*, **2013**, 270, 49-57.
89. Davila, Y.; Petitmangin, A.; Hebert, C.; Perriere, J.; Seiler, W. Oxygen deficiency in oxide films grown by PLD. *Applied Surface Science*, **2011**, 257(12), 5354-5357.
90. Socol, G.; Gnatyuk, Y.; Stefan, N.; Smirnova, N.; Djokic, V.; Sutan, C.; Malinovschi, V.; Stanculescu, A.; Korduban, O.; Mihailescu, I.N. Photocatalytic activity of pulsed laser deposited TiO_2 thin films in N_2, O_2 and CH_4. *Thin Solid Films*, **2010**, 518(16), 4648-4653.
91. Nath, A.; Laha, S.S.; Khare, A. Effect of focusing conditions on synthesis of titanium oxide nanoparticles via laser ablation in titanium-water interface. *Applied Surface Science*, **2011**, 257(7), 3118-3122.
92. Rahman, M.A.; Bazargan, S.; Srivastava, S.; Wang, X.; Abd-Ellah, M.; Thomas, J.P.; Heinig, N.F.; Pradhan, D.; Leung, K.T. Defect-rich decorated TiO_2 nanowires for super-efficient photoelectrochemical water splitting driven by visible light. *Energy & Environmental Science*, **2015**, 8(11), 3363-3373.
93. Bellardita, M.; Garlisi, C.; Ozer, L.Y.; Venezia, A.M.; Sa, J.; Mamedov, F.; Palmisano, L.; Palmisano, G. Highly stable defective TiO_{2-x} with tuned exposed facets induced by fluorine: Impact of surface and bulk properties on selective UV/visible alcohol photo-oxidation. *Applied Surface Science*, **2020**, 510, 145419.
94. Lo, H.H.; Gopal, N.O.; Ke, S.C. Origin of photoactivity of oxygen-deficient TiO_2 under visible light. *Applied Physics Letters*, **2009**, 95(8) 083126.
95. Pu, X.; Hu, Y.; Cui, S.; Cheng, L.; Jiao, Z. Preparation of N-doped and oxygen-deficient TiO_2 microspheres via a novel electron beam-assisted method. *Solid State Sciences*, **2017**, 70, 66-73.
96. Wang, M.; Xu, X.Y.; Lin, L.; He, D.N. Gd-La codoped TiO_2 nanoparticles as solar photocatalysts. *Progress in Natural Science-Materials International*, **2015**, 25 (1), 6-11.
97. Kunti, A.K.; Sharma, S.K. Structural and spectral properties of red light emitting Eu^{3+} activated TiO_2 nanophosphor for white LED application. *Ceramics International*, **2017**, 43(13), 9838-9845.
98. Zhang, J.W.; Zhang, J.W.; Ren, H.H.; Yu, L.G.; Wu, Z.S.; Zhang, Z.J. High rate capability and long cycle stability of TiO_2-delta-La composite nanotubes as anode material for lithium ion batteries. *Journal of Alloys and Compounds*, **2014**, 609, 178-184.
99. Zhang, J.Y.; Zhao, Z.Y.; Wang, X.Y.; Yu, T.; Guan, J.; Yu, Z.T.; Li, Z.S.;Zou, Z.G. Increasing the oxygen vacancy density on the TiO_2 surface by la-doping for dye-sensitized solar cells. *Journal of Physical Chemistry C*, **2010,** 114(43), 18396-18400.
100. Hatanaka, Y.; Naito, H.; Itou, S.; Kando, M. Photocatalytic characteristics of hydro-oxygenated amorphous titanium oxide films prepared using remote plasma enhanced chemical vapor deposition. *Applied Surface Science*, **2005**, 244 (1-4), 554-557.
101. Sakai, T.; Kuniyoshi, Y.; Aoki, W.; Ezoe, S.; Endo, T.; Hoshi, Y. High-rate deposition of photocatalytic TiO_2 films by oxygen plasma assist reactive evaporation method. *Thin Solid Films*, **2008**, 516(17), 5860-5863.
102. Li, Y.; Wang, W.; Wang, F.; Di, L.; Yang, S.; Zhu, S.; Yao, Y.; Ma, C.; Dai, B.; Yu, F. Enhanced photocatalytic degradation of organic dyes via defect-rich TiO_2 prepared by dielectric barrier discharge plasma. *Nanomaterials*, **2019**, 9(5), 720.
103. Hojo, M.; Okimura, K. Effect of annealing with ar plasma irradiation for transparent conductive Nb-doped TiO_2 films on glass substrate. *Japanese Journal of Applied Physics*, **2009**, 48(8), 08HK06.
104. Kawakami, R.; Mimoto, Y.; Yanagiya, S.i.; Shirai, A.; Niibe, M.; Nakano, Y.; Mukai, T. Photocatalytic activity enhancement of anatase/rutile-mixed phase TiO_2 nanoparticles annealed with low-temperature O_2 plasma. *Physica Status Solidi a-Applications and Materials Science*, **2021**, 218(24), 2100536.
105. An, H.R.; Hong, Y.C.; Kim, H.; Huh, J.Y.; Park, E.C.; Park, S.Y.; Jeong, Y.; Park, J.I.; Kim, J.P.; Lee, Y.C.; Hong, W.K.; Oh, Y.K.; Kim, Y.J.; Yang, M.; Lee, H.U. Studies on mass production and highly solar light photocatalytic properties of gray hydrogenated-TiO_2 sphere photocatalysts. *Journal of Hazardous Materials*, **2018**, 358, 222-233.
106. Mizukoshi, Y.; Ohwada, M.; Seino, S.; Horibed, H.; Nishimura, Y.; Terashima, C. Synthesis of oxygen-deficient blue titanium oxide by discharge plasma generated in aqueous ammonia solution. *Applied Surface Science*, **2019**, 489,255-261.
107. Ji, M.; Choa, Y.H.; Lee, Y.I. One-step synthesis of black TiO_{2-x} microspheres by ultrasonic spray pyrolysis process and their visible-light-driven photocatalytic activities. *Ultrasonics Sonochemistry*, **2021**, 74, 105557.
108. Nakaruk, A.; Reece, P.J.; Ragazzon, D.; Sorrell, C.C. TiO_2 films prepared by ultrasonic spray pyrolysis. *Materials Science and Technology*, **2010**, 26(4), 469-472.
109. Osorio-Vargas, P.A.; Pulgarin, C.; Sienkiewicz, A.; Pizzio, L.R.; Blanco, M.N.; Torres-Palma, R.A.; Petrier, C .; Rengifo-Herrera, J.A. Low-frequency ultrasound induces oxygen vacancies formation and visible light absorption in TiO_2 P-25 nanoparticles. *Ultrasonics Sonochemistry*, **2012**, 19(3), 383-386.

110. Bellardita, M.; El Nazer, H.A.; Loddo, V.; Parrino, F.; Venezia, A.M.; Palmisano, L. Photoactivity under visible light of metal loaded TiO_2 catalysts prepared by low frequency ultrasound treatment. *Catalysis Today*, **2017**, *284*, 92-99.
111. Langhammer, D.; Thyr, J.; Osterlund, L. Surface properties of reduced and stoichiometric TiO_2 as probed by SO_2 adsorption. *Journal of Physical Chemistry C*, **2019**, 123(40), 24549-24557.
112. Xu, M.; Chen, Y.; Qin, J.; Feng, Y.; Li, W.; Chen, W.; Zhu, J.; Li, H.; Bian, Z. Unveiling the role of defects on oxygen activation and photodegradation of organic pollutants. *Environmental Science & Technology*, **2018**, 52(23), 13879-13886.
113. Albetran, H.; O'Connor, B.H.; Low, I.M. Effect of calcination on band gaps for electrospun titania nanofibers heated in air-argon mixtures. *Materials & Design*, **2016**, 92, 480-485.
114. Sang, L.X.; Zhang, Z.Y.; Ma, C.F. Photoelectrical and charge transfer properties of hydrogen-evolving TiO_2 nanotube arrays electrodes annealed in different gases. *International Journal of Hydrogen Energy*, **2011**, 36(8), 4732-4738.
115. Qi, W.; Zhang, F.; An, X.; Liu, H.; Qu, J. Oxygen vacancy modulation of {010}-dominated TiO_2 for enhanced photodegradation of Sulfamethoxazole. *Catalysis Communications*, **2019**, 118, 35-38.
116. Li, Y.; Ye, X.; Cao, S.; Yang, C.; Wang, Y.; Ye, J. Oxygen-Deficient Dumbbell-Shaped Anatase TiO_{2-x} Mesocrystals with Nearly 100% Exposed {101} Facets: Synthesis, Growth Mechanism, and Photocatalytic Performance. *Chemistry-a European Journal*, **2019**, 25(12), 3032-3041.
117. Du, M.; Chen, Q.; Wang, Y.; Hu, J.; Meng, X. Synchronous construction of oxygen vacancies and phase junction in TiO_2 hierarchical structure for enhancement of visible light photocatalytic activity. *Journal of Alloys and Compounds*, **2020**, 830, 154649.
118. Sheng, Z.; Song, S.; Wang, H.; Wu, Z.; Liu, Y. One-step hydrothermal synthesis of Pd-modified TiO_2 with high photocatalytic activity for nitric oxide oxidation in gas phase. *Environmental Engineering Science*, **2012**, 29(10), 972-978.
119. Sasirekha, N.; Basha, S.J.S.; Shanthi, K. Photocatalytic performance of Ru doped anatase mounted on silica for reduction of carbon dioxide. *Applied Catalysis B-Environmental*, **2006**, 62(1-2), 169-180.
120. Gao, P.; Yang, L.; Xiao, S.; Wang, L.; Guo, W.; Lu, J. Effect of Ru, Rh, Mo, and Pd adsorption on the electronic and optical properties of anatase TiO_2 (101): A DFT Investigation. *Materials*, **2019**, 12(5), 814.
121. Thalgaspitiya, W.R.K.; Kapuge, T.K.; He, J.; Deljoo, B.; Meguerdichian, A.G.; Aindow, M.; Suib, S.L. Multifunctional transition metal doped titanium dioxide reduced graphene oxide composites as highly efficient adsorbents and photocatalysts. *Microporous and Mesoporous Materials*, **2020**, 307, 110521.
122. Wang, T.; Li, B.R.; Wu, L.G.; Yin, Y.B.; Jiang, B.Q.; Lou, J.Q. Enhanced performance of TiO_2/reduced graphene oxide doped by rare-earth ions for degrading phenol in seawater excited by weak visible light. *Advanced Powder Technology*, **2019**, 30(9), 1920-1931.
123. Stengl, V.; Bakardjieva, S.; Murafa, N. Preparation and photocatalytic activity of rare earth doped TiO_2 nanoparticles. *Materials Chemistry and Physics*, **2009**, 114(1), 217-226.
124. Fang, X.L.; Chen, X.H.; Zhu, Z.S. Optical and photocatalytic properties of Er^{3+} and/or Yb^{3+} doped TiO_2 photocatalysts. *Journal of Materials Science-Materials in Electronics*, **2017**, 28(1), 474-479.
125. Setiawati, E.; Kawano, K. Stabilization of anatase phase in the rare earth; Eu and Sm ion doped nanoparticle TiO_2. *Journal of Alloys and Compounds*, **2008**, 451(1-2), 293-296.
126. Yu, Y.G.; Chen, G.; Zhou, Y.S.; Han, Z.H. Recent advances in rare-earth elements modification of inorganic semiconductor-based photocatalysts for efficient solar energy conversion: A review. *Journal of Rare Earths*, **2015**, 33(5), 453-462.
127. Liu, S.Y.; Zuo, C.G.; Xia, J. Solid-state synthesis and photodegradation property of anatase TiO_2 micro-nanopowder by sodium replacement. *Solid State Sciences*, **2021**, 115, 106589.
128. Lv, C.; Lan, X.; Wang, L.; Yu, Q.; Zhang, M.; Sun, H.; Shi, J. Alkaline-earth-metal-doped TiO_2 for enhanced photodegradation and H_2 evolution: insights into the mechanisms. *Catalysis Science & Technology*, **2019**, 9(21), 6124-6135.
129. Li, H.; Hao, Y.B.; Lu, H.Q.; Liang, L.; Wang, Y.; Qiu, J.H.; Shi, X.; Wang, Y.Y.; Yao, J.F. systematic study on visible-light N-doped TiO_2 photocatalyst obtained from ethylenediamine by sol-gel method. *Applied Surface Science*, **2015**, 344, 112-118.
130. Chaudhari, N.S.; Warule, S.S.; Dhanmane, S.A.; Kulkarni, M.V.; Valant, M.; Kale, B.B. Nanostructured N-doped TiO_2 marigold flowers for an efficient solar hydrogen production from H_2S. *Nanoscale*, **2013**, 5(19), 9383-9390.
131. Wang, Y.W.; Huang, Y.; Ho, W.K.; Zhang, L.; Zou, Z.G.; Lee, S.C. Biomolecule-controlled hydrothermal synthesis of C-N-S-tridoped TiO_2 nanocrystalline photocatalysts for NO removal under simulated solar light irradiation. *Journal of Hazardous Materials*, **2009**, 169(1-3), 77-87.
132. Li, Y.X.; Ma, GF..; Peng, S.; Lu, G.; Li, S.B. Boron and nitrogen co-doped titania with enhanced visible-light photocatalytic activity for hydrogen evolution. *Applied Surface Science*, **2008**, 254(21), 6831-6836.

133. Yuan, J.; Chen, M.X.; Shi, J.W.; Shangguan, W.F. Preparations and photocatalytic hydrogen evolution of N-doped TiO_2 from urea and titanium tetrachloride. *International Journal of Hydrogen Energy*, **2006**, 31(10), 1326-1331.
134. Momeni, M.M.; Ghayeb, Y.; Ghonchegi, Z. Visible light activity of sulfur-doped TiO_2 nanostructure photoelectrodes prepared by single-step electrochemical anodizing process. *Journal of Solid State Electrochemistry*, **2015**, 19(5), 1359-1366.
135. Carmichael, P.; Hazafy, D.; Bhachu, D.S.; Mills, A.; Darr, J.A.; Parkin, I.P. Atmospheric pressure chemical vapour deposition of boron doped titanium dioxide for photocatalytic water reduction and oxidation. *Physical Chemistry Chemical Physics*, **2013**, *15* (39), 16788-16794.
136. Wu, G.S.; A. Chen. Direct growth of F-doped TiO_2 particulate thin films with high photocatalytic activity for environmental applications. *Journal of Photochemistry and Photobiology a-Chemistry*, **2008**, 195(1), 47-53.
137. Zhu, H.X.; Liu, J.M. First principles calculations of electronic and optical properties of Mo and C co-doped anatase TiO_2. *Applied Physics a-Materials Science & Processing*, **2014**, 117(2), 831-839.
138. Diao, W.Y.; He, J.; Wang, Q.; Rao, X.; Zhang, Y.P. K, Na and Cl co-doped TiO_2 nanorod arrays on carbon cloth for efficient photocatalytic degradation of formaldehyde under UV/visible LED irradiation. *Catalysis Science & Technology*, **2021**, 11(1), 230-238.
139. Barakat, N.A.M.; Zaki, A.H.; Ahmed, E.; Farghali, A.A.; Al-Mubaddel, F.S. Fe_xCo_{1-x}-doped titanium oxide nanotubes as effective photocatalysts for hydrogen extraction from ammonium phosphate. *International Journal of Hydrogen Energy*, **2018**, 43(16), 7990-7997.
140. Filippatos, P.P.; Soultati, A.; Kelaidis, N.; Petaroudis, C.; Alivisatou, A.A.; Drivas, C.; Kennou, S.; Agapaki, E.; Charalampidis, G.; Yusoff, A.R.b.M.; Lathiotakis, N.N.; Coutsolelos, A.G.; Davazoglou, D.; Vasilopoulou, M.; Chroneos, A. Preparation of hydrogen, fluorine and chlorine doped and co-doped titanium dioxide photocatalysts: a theoretical and experimental approach. *Scientific Reports*, **2021**, 11(1), 5700.
141. Meng, S.G.; Zhang, J.F.; Chen, S.F.; Zhang, S.J.; Huang, W.X. Perspective on construction of heterojunction photocatalysts and the complete utilization of photogenerated charge carriers. *Applied Surface Science*, **2019**, *476*, 982-992.
142. Low, J.X.; Yu, J.G.; Jaroniec, M.; Wageh, S.; Al-Ghamdi, A.A. Heterojunction photocatalysts. *Advanced Materials*, **2017**, 29(20), 1601694.
143. Smith, Y.R.; Sarma, B.; Mohanty, S.K.; Misra, M. Formation of TiO_2-WO_3 nanotubular composite via single-step anodization and its application in photoelectrochemical hydrogen generation. *Electrochemistry Communications*, **2012**, 19, 131-134.
144. Choudhury, S.; Sasikala, R.; Saxena, V.; Aswal, D.K.; Bhattacharya, D. A new route for the fabrication of an ultrathin film of a PdO-TiO_2 composite photocatalyst. *Dalton Transactions*, **2012**, 41(39), 12090-12095.
145. Navarrete, M.; Cipagauta-Diaz, S.; Gomez, R. Ga_2O_3/TiO_2 semiconductors free of noble metals for the photocatalytic hydrogen production in a water/methanol mixture. *Journal of Chemical Technology and Biotechnology*, **2019**, 94(11), 3457-3465.
146. Gholami, M.; Shirzad-Siboni, M.; Farzadkia, M.; Yang, J.K. Synthesis, characterization, and application of ZnO/TiO_2 nanocomposite for photocatalysis of a herbicide (Bentazon). *Desalination and Water Treatment*, **2016**, 57(29), 13632-13644.
147. Chen, J.Z.; Chen, T.H.; Lai, L.W.; Li, P.Y.; Liu, H.W.; Hong, Y.Y.; Liu, D.S. Preparation and characterization of surface photocatalytic activity with NiO/TiO_2 nanocomposite structure. *Materials*, **2015**, 8(7),4273-4286.
148. Wang, W.T.; Wu, Z.Q.; Eftekhari, E.; Huo, Z.Y.; Li, X.M.; Tade, M.O.; Yan, C.; Yan, Z.F.; Li, C.H.; Li, Q.; Zhao, D.Y. High performance heterojunction photocatalytic membranes formed by embedding Cu_2O and TiO_2 nanowires in reduced graphene oxide. *Catalysis Science & Technology*, **2018**, 8(6), 1704-1711.
149. Morales-Torres, S.; Pastrana-Martinez, L.M.; Figueiredo, J.L.; Faria, J.L.; Silva, A.M.T. Design of graphene-based TiO_2 photocatalysts-a review. *Environmental Science and Pollution Research*, **2012**, 19(9), 3676-3687.
150. Gao, P.; Sun, D.D. ultrasonic preparation of hierarchical graphene-oxide/TiO_2 composite microspheres for efficient photocatalytic hydrogen production. *Chemistry-an Asian Journal*, **2013**, 8(11), 2779-2786.
151. Kong, D.W.; Zhao, M.; Li, S.K.; Huang, F.; Song, J.M.; Yuan, Y.P.; Shen, Y.H.; Xie, A.J. Synthesis of TiO_2/rGO nanocomposites with enhanced photoelectrochemical performance and photocatalytic activity. *Nano*, **2016**, 11(1), 1650007.
152. Zhang, X.Y.; Li, H.P.; Cui, X.L. Preparation and photocatalytic activity for hydrogen evolution of TiO_2/graphene sheets composite. *Chinese Journal of Inorganic Chemistry*, **2009**, 25(11), 1903-1907.
153. Shen, J.F; Shi, M.; Yan, B.; Ma, H.W.; Li, N.; Ye, M.X. Ionic liquid-assisted one-step hydrothermal synthesis of TiO_2-reduced graphene oxide composites. *Nano Research*, **2011**, 4(8), 795-806.
154. Fu, Z.; Wang, H.; Wang, Y.N.; Wang, S.H.; Li, Z.L.; Sun, Q. Construction of three-dimensional g-C_3N_4/Gr-CNTs/TiO_2 Z-scheme catalyst with enhanced photocatalytic activity. *Applied Surface Science*, **2020**, 510, 145494.

155. Chiang, H.H.; Wang, S.H.; Chou, H.Y.; Huang, C.C.; Tsai, T.L.; Yang, Y.C.; Lee, J.W.; Lin, T.Y.; Wu, Y.J.; Chen, C.C.. Surface modification of ato photocatalyst on its bactericidal effect against escherichia coli. *Journal of Marine Science and Technology-Taiwan*, **2014**, *22* (2), 2014, 22(2): 269-276.
156. Zhou, X.M. TiO_2-supported single-atom catalysts for photocatalytic reactions. *Acta Physico-Chimica Sinica*, **2021**, 37(6), 2008064.
157. Bernareggi, M.; Chiarello, G.L.; West, G.; Ratova, M.; Ferretti, A.M.; Kelly, P.; Selli, E. Cu and Pt clusters deposition on TiO_2 powders by DC magnetron sputtering for photocatalytic hydrogen production. *Catalysis Today*, **2019**, 326, 15-21.
158. Dozzi, M.V.; Brocato, S.; Marra, G.; Tozzola, G.; Meda, L.; Selli, E. Aqueous ammonia abatement on Pt- and Ru-modified TiO_2: Selectivity effects of the metal nanoparticles deposition method. *Catalysis Today*, **2017**, 287, 148-154.
159. Zheng, Z.; Murakamia, N.; Liu, J.J.; Teng, Z.; Zhang, Q.T.; Cao, Y.; Cheng, H.H.; Ohno, T. Development of plasmonic photocatalyst by site-selective loading of bimetallic nanoparticles of Au and Ag on titanium(IV) oxide. *Chemcatchem*, **2020**, 12(14), 3783-3792.
160. Luo, J.; Li, D.L.; Yang, Y.; Liu, H.Q.; Chen, J.Y.; Wang, H.Y. Preparation of Au/reduced graphene oxide/hydrogenated TiO_2 nanotube arrays ternary composites for visible-light-driven photoelectrochemical water splitting. *Journal of Alloys and Compounds*, **2016**, 661, 380-388.
161. Ge, M.Z.; Cao, C.Y.; Li, S.H.; Tang, Y.X.; Wang, L.N.; Qi, N.; Huang, J.Y.; Zhang, K.Q.; Al-Deyab, S.S.; Lai, Y.K. In situ plasmonic Ag nanoparticle anchored TiO_2 nanotube arrays as visible-light-driven photocatalysts for enhanced water splitting. *Nanoscale*, **2016**, 8(9), 5226-5234.
162. Liu, E.Z.; Kang, L.M.; Yang, Y.; Sun, T.; Hu, X.Y.; Zhu, C.; Liu, H.C.; Wang, Q.P.; Li, X.H.; Fan, J. Plasmonic Ag deposited TiO_2 nano-sheet film for enhanced photocatalytic hydrogen production by water splitting. *Nanotechnology*, **2014**, 25(16) 165401.
163. Barrios, C.E.; Albiter, E.; Jimenez, J.; Tiznado, H.; Romo-Herrera, J.; Zanella, R. Photocatalytic hydrogen production over titania modified by gold - Metal (palladium, nickel and cobalt) catalysts. *International Journal of Hydrogen Energy*, **2016**, 41 (48), 23287-23300.
164. Monamary, A.; Vijayalakshmi, K. Substantial effect of palladium overlayer deposition on the H_2 sensing performance of TiO_2/ITO nanocomposite. *Ceramics International*, **2018**, 44(18), 22957-22962.
165. Shi, J.W.; Guan, X.J.; Zhou, Z.H.; Liu, H.P.; Guo, L.J. Eosin Y-sensitized nanosheet-stacked hollow-sphere TiO_2 for efficient photocatalytic H_2 production under visible-light irradiation. *Journal of Nanoparticle Research*, **2015**, 17(6) 252.
166. Murcia, J.J.; Avila-Martinez, E.G.; Rojas, H.; Cubillos, J.; Ivanova, S.; Penkova, A.; Laguna, O.H. Powder and nanotubes titania modified by dye sensitization as photocatalysts for the organic pollutants elimination. *Nanomaterials*, **2019**, *9* (4) 517.
167. Vallejo, W.; Rueda, A.; Diaz-Uribe, C.; Grande, C.; Quintana, P. Photocatalytic activity of graphene oxide-TiO_2 thin films sensitized by natural dyes extracted from Bactris guineensis. *Royal Society Open Science*, **2019**, 6(3) 181824.
168. Rodriguez, H.B.; Di Iorio, Y.; Meichtry, J.M.; Grela, M.A.; Litter, M.I.; San Roman, E. Evidence on dye clustering in the sensitization of TiO_2 by aluminum phthalocyanine. *Photochemical & Photobiological Sciences*, **2013**, 12(11), 1984-1990.
169. Ding, H.M.; Sun, H.; Shan, Y.K. Preparation and characterization of mesoporous SBA-15 supported dye-sensitized TiO_2 photocatalyst. *Journal of Photochemistry and Photobiology a-Chemistry*, **2005**, 169(1), 101-107.
170. Wahyuningsih, S.; Purnawan, C.; Kartikasari, P.A.; Praistia, N. Visible light photoelectrocatalytic degradation of rhodamine B using a dye-sensitised TiO_2 electrode. *Chemical Papers*, **2014**, 68(9), 1248-1256.
171. Li, Y.; Li, H.M.; Lu, X.L.; Yu, X.; Kong, M.H.; Duan, X.D.; Qin, G.; Zhao, Y.H.; Wang, Z.L.; Dionysiou, D.D. Molybdenum disulfide nanosheets vertically grown on self-supported titanium dioxide/nitrogen-doped carbon nanofiber film for effective hydrogen peroxide decomposition and "memory catalysis". *Journal of Colloid and Interface Science*, **2021,** 596, 384-395.
172. Ikeue, K.; Yamashita, H.; Anpo, M. Photocatalytic reduction of CO_2 with H_2O on titanium oxides prepared within zeolites and mesoporous molecular sieves. *Electrochemistry*, **2002**, 70(6), 402-408.
173. Rasalingam, S.; Kibombo, H.S.; Wu, C.M.; Budhi, S.; Peng, R.; Baltrusaitis, J.; Koodali, R.T. Influence of Ti-O-Si hetero-linkages in the photocatalytic degradation of Rhodamine B. *Catalysis Communications*, **2013**, 31, 66-70.
174. Liu, B.; Zeng, H.C. Carbon nanotubes supported mesoporous mesocrystals of anatase TiO_2. *Chemistry of Materials*, **2008**, 20(8), 2711-2718.
175. Najafabadi, A.T.; Taghipour, F. Physicochemical impact of zeolites as the support for photocatalytic hydrogen production using solar-activated TiO_2-based nanoparticles. *Energy Conversion and Management*, **2014**, 82, 106-113.
176. Xu, Y.M.; Langford, C.H. Enhanced photoactivity of a titanium(iv) oxide-supported on ZSM5 and zeolite-a at low-coverage. *Journal of Physical Chemistry*, **1995**, 99(29), 11501-11507.

177. Kim, H.J.; Shul, Y.G.; Han, H.S. Photocatalytic properties of silica-supported TiO_2. *Topics in Catalysis*, **2005**, *35* (3-4), 287-293.
178. Yin, J.W.; Xing, Z.P.; Kuang, J.Y.; Li, Z.Z.; Li, M.; Jiang, J.J.; Tan, S.Y.; Zhu, Q.; Zhou, W. Bi plasmon-enhanced mesoporous Bi_2MoO_6/Ti^{3+} self-doped TiO_2 microsphere heterojunctions as efficient visible-light-driven photocatalysts. *Journal of Alloys and Compounds*, **2018**, 750, 659-668.
179. Xing, M.Y.; Zhang, J.L.; Qiu, B.C.; Tian, B.Z.; Anpo, M.; Che, M. A brown mesoporous TiO_{2-x}/MCF Composite with an extremely high quantum yield of solar energy photocatalysis for H_2 evolution. *Small*, **2015**, 11(16), 1920-1929.
180. Wen, C.Z.; Jiang, H.B.; Qiao, S.Z.; Yang, H.G.; Lu, G.Q. Synthesis of high-reactive facets dominated anatase TiO_2. *Journal of Materials Chemistry*, **2011**, 21(20), 7052-7061.
181. Li, H.M.; Zeng, Y.S.; Huang, T.C.; Piao, L.; Liu, M. Controlled synthesis of anatase TiO_2 single crystals with dominant {001} facets from TiO_2 powders. *Chempluschem*, **2012**, 77(11), 1017-1021.
182. Wang, W.; Lu, C.H.; Ni, Y.R.; Song, J.B.; Su, M.X.; Xu, Z.Z. Enhanced visible-light photoactivity of {001} facets dominated TiO_2 nanosheets with even distributed bulk oxygen vacancy and Ti^{3+}. *Catalysis Communications*, **2012**, 22, 19-23.
183. Shang, Q.Q.; Tan, X.; Yu, T.; Zhang, Z.Y.; Zou, Y.; Wang, S.Y. Efficient gaseous toluene photoconversion on graphene-titanium dioxide nanocomposites with dominate exposed {001} facets. *Journal of Colloid and Interface Science*, **2015**, 455, 134-144.
184. Lv, Z.G.; Cheng, X.; Liu, B.Q.; Guo, Z.M.; Jin, M.M.; Zhang, C. Enhanced photoredox water splitting of Sb-N donor-acceptor pairs in TiO_2. *Inorganic Chemistry Frontiers*, **2019**, 6(9), 2404-2411.
185. Koci, K.; Troppova, I.; Edelmannova, M.; Starostka, J.; Matejova, L.; Lang, J.; Reli, M.; Drobna, H.; Rokicinska, A.; Kustrowski, P.; Capek, L. Photocatalytic decomposition of methanol over La/TiO_2 materials. *Environmental Science and Pollution Research*, **2018**, 25(35), 34818-34825.
186. Bharatvaj, J.; Preethi, V.; Kanmani, S. Hydrogen production from sulphide wastewater using Ce^{3+}-TiO_2 photocatalysis. *International Journal of Hydrogen Energy*, **2018**, 43(8), 3935-3945.
187. Agegnehu, A.K.; Pan, C.J.; Tsai, M.C.; Rick, J.; Su, W.N.; Lee, J.F.; Hwang, B.J. Visible light responsive noble metal-free nanocomposite of V-doped TiO_2 nanorod with highly reduced graphene oxide for enhanced solar H_2 production. *International Journal of Hydrogen Energy*, **2016**, 41(16), 6752-6762.
188. Barakat, N.A.M.; Ahmed, E.; Amen, M.T.; Abdelkareem, M.A.; Farghali, A.A. N-doped Ni/C/TiO_2 nanocomposite as effective photocatalyst for water splitting. *Materials Letters*, **2018**, 210,317-320.
189. Gao, L.S.; Zhang, S.N.; Zou, X.X.; Wang, J.F.; Su, J.; Chen, J.S. Oxygen vacancy engineering of titania-induced by Sr^{2+} dopants for visible-light-driven hydrogen evolution. *Inorganic Chemistry*, **2021**, 60(1), 32-36.
190. Xu, J.C.; Zhang, J.J.; Cai, Z.Y.; Huang, H.; Huang, T.H.; Wang, P.; Wang, X.Y. Facile and large-scale synthesis of defective black TiO_{2-x}(B) nanosheets for efficient visible-light-driven photocatalytic hydrogen evolution. *Catalysts*, **2019**, 9(12), 1048.
191. Barakat, N.A.M.; Erfan, N.A.; Mohammed, A.A.; Mohamed, S.E.I. Ag-decorated TiO_2 nanofibers as Arrhenius equation-incompatible and effective photocatalyst for water splitting under visible light irradiation. *Colloids and Surfaces a-Physicochemical and Engineering Aspects*, **2020**, 604, 125307.
192. Dang, H.F.; Dong, X.F.; Dong, Y.C.; Zhang, Y.; Hampshire, S. TiO_2 nanotubes coupled with nano-$Cu(OH)_2$ for highly efficient photocatalytic hydrogen production. *International Journal of Hydrogen Energy*, **2013**, 38(5), 2126-2135.
193. Diaz, L.; Rodriguez, V.D.; Gonzalez-Rodriguez, M.; Rodriguez-Castellon, E.; Algarra, M.; Nunez, P.; Moretti, E. M/TiO_2 (M = Fe, Co, Ni, Cu, Zn) catalysts for photocatalytic hydrogen production under UV and visible light irradiation. *Inorganic Chemistry Frontiers*, **2021**, 8(14), 3491-3500.
194. El-Bery, H.M.; Abdelhamid, H.N. Abdelhamid. Photocatalytic hydrogen generation via water splitting using ZIF-67 derived Co_3O_4@C/TiO_2. *Journal of Environmental Chemical Engineering*, **2021**, 9(4), 105702.
195. Fujita, S.; Kawamori, H.; Honda, D.; Yoshida, H.; Arai, M. Photocatalytic hydrogen production from aqueous glycerol solution using NiO/TiO_2 catalysts: Effects of preparation and reaction conditions. *Applied Catalysis B-Environmental*, **2016**, 181, 818-824.
196. Kokporka, L.; Onsuratoom, S.; Puangpetch, T.; Chavadej, S. Sol-gel-synthesized mesoporous-assembled TiO_2-ZrO_2 mixed oxide nanocrystals and their photocatalytic sensitized H_2 production activity under visible light irradiation. *Materials Science in Semiconductor Processing*, **2013**, 16(3), 667-678.
197. Mou, Z.G.; Wu, Y.J.; Sun, J.H.; Yang, P.; Du, Y.K.; Lu, C. TiO_2 Nanoparticles-functionalized N-doped graphene with superior interfacial contact and enhanced charge separation for photocatalytic hydrogen generation. *ACS Applied Materials & Interfaces*, **2014**, 6(16), 13798-13806.
198. Sharma, A.; Thuan, D.V.; Pham, T.D.; Tung, M.H.T.; Truc, N.T.T.; Vo, D.V.N. Advanced surface of fibrous activated carbon immobilized with FeO/TiO_2 for photocatalytic evolution of hydrogen under visible light. *Chemical Engineering & Technology*, **2020**, 43(4), 752-761.
199. Wang, C.; Hu, Q.Q.; Huang, J.Q.; Zhu, C.; Deng, Z.H.; Shi, H.L.; Wu, L.; Liu, Z.G.; Cao, Y.G. Enhanced hydrogen production by water splitting using Cu-doped TiO_2 film with preferred (001) orientation. *Applied Surface Science*, **2014**, 292, 161-164.

200. Ma, J.; Tan, X.L.; Yu, T.; Li, X. Fabrication of g-C_3N_4/TiO_2 hierarchical spheres with reactive {001} TiO_2 crystal facets and its visible-light photocatalytic activity. *International Journal of Hydrogen Energy*, **2016**, 41(6), 3877-3887.
201. Xiang, Q.J.; Yu, J.G.; Jaroniec, M. Enhanced photocatalytic H_2 production activity of graphene-modified titania nanosheets. *Nanoscale*, **2011**, 3(9), 3670-3678.